**Amine-Functionalized MCM-41/Polysulfone Mixed Matrix Membranes:**

**Preparation, Characterization and Its Performance in $CO_2/CH_4$ Separation**

by

Foo Khai Zhen

14869

Dissertation submitted in partial fulfillment of

the requirements for the

Bachelor of Engineering (Hons)

(Chemical Engineering)

January 2015

Universiti Teknologi PETRONAS

Bandar Seri Iskandar

31750 Tronoh

Perak Darul Ridzuan

CERTIFICATION OF APPROVAL

**Amine-Functionalized MCM-41/Polysulfone Mixed Matrix Membranes:**

**Preparation, Characterization and Its Performance in $CO_2/CH_4$ Separation**

by

Foo Khai Zhen

14869

A project dissertation submitted to the

Chemical Engineering Programme

Universiti Teknologi PETRONAS

in partial fulfilment of the requirement for the

BACHELOR OF ENGINEERING (Hons)

(CHEMICAL)

Approved by,

_____

(Dr. Yeong Yin Fong)

UNIVERSITI TEKNOLOGI PETRONAS

TRONOH, PERAK

January 2015

This is to certify that I am responsible for the work submitted in this project, that the original work is my own except as specified in the references and acknowledgements, and that the original work contained herein have not been undertaken or done by unspecified sources or persons.

_____

(Foo Khai Zhen)

# ABSTRACT

Mixed matrix membrane or MMM, comprising polymeric membrane and inorganic fillers, is promising in gas separation as it combines the advantages of the two components. However, the fabrication of MMM is challenging due to the issue of agglomeration of inorganic fillers and the formation of interfacial voids on MMM surface morphology. Nevertheless, the dispersion of the filler and interaction between filler-polymer can be improved by modifying filler with binding agents, which improves the separation performance of MMM. This work is about synthesis and characterization of new modified fillers to be used in MCM-41/Psf MMM for $CO_2/CH_4$ separation. Mesoporous MCM-41 silica is modified with primary (APTMS) and secondary amine functional groups (AAPTMS) using grafting method. MMMs with MCM-41, APTMS-MCM-41 and AAPTMS-MCM-41 were synthesized using dry/wet inversion method. The filler loadings were set as 0.1 wt% and 1 wt%. The synthesized MMMs were characterized using TEM, SEM, FT-IR and EDX. The $CO_2/CH_4$ separation performance of MMMs was tested using gas permeation test rig, where the permeance and selectivity of MMMs were compared to pure Psf membrane. TEM results showed reduction of particles agglomeration after amine functionalization. Besides, the hexagonal structure of MCM-41 remained intact after functionalization. Based on the results obtained from SEM and EDX, the fillers were uniformly dispersed in the Psf matrix, while the presence of amine functional groups APTMS and AAPTMS on MCM-41 has improved the compatibility between fillers and matrix. FT-IR results confirmed the successful grafting of the amine groups on MCM-41 at the band of ~690 $cm^{-1}$ and ~1530$cm^{-1}$. The incorporation of APTMS-MCM-41 into Psf has successfully increased the $CO_2$ permeability by 410.44% (0.1 wt% loading) and 569.97% (1 wt% loading), while AAPTMS-MCM-41 has 114.10% (0.1 wt% loading) and 309.32% (0.1 wt% loading). APTMS-MCM-41 has better overall performance than AAPTMS-MCM-41 in terms of permeance. All MMMs showed an inverse relationship between permeance and ideal selectivity as indicated by Robeson's trade-off bound.

# ACKNOWLEDGEMENT

First and foremost, I would like to express my deepest gratitude to my supervisor Dr. Yeong Yin Fong for her patient guidance and support throughout the semester which made me possible to carry out this project. Her attentive supervision and guidance is much appreciated.

I would also like to thank all lecturers from Universiti Teknologi PETRONAS who had guided me throughout the period of the project. Furthermore, thanks to the assistance of PHD and matster students, Muhammad Mubashir, Lai Li Sze, Wahyu Wahlah and Sarah Mohammad, in providing additional information for the project.

In addition, I thank my family members and fellow friends who gave moral support in completing this project. Next, special thanks to the advice and support of FYP coordinator and FYP examiner, this thesis has turned out to be a successful and meaningful paper for fundamental research understanding of mixed matrix membranes. Lastly, my gratitude goes to the Chemical Engineering Department of Universiti Teknologi PETRONAS (UTP) for providing us the chance to undertake Final Year Project I and II.

**TABLE OF CONTENTS**

# LIST OF FIGURES

# LIST OF TABLES

# CHAPTER 1

# INTRODUCTION

## 1. INTRODUCTION

### 1.1 Background of Study

Natural gas is the largest industrial gas separation application by far with increasing consumption in the world yearly. In natural gas, methane ($CH_4$) is the primary component (typically 90%), along with some ethane and propane. Carbon dioxide ($CO_2$) is found as impurity most of the time. $CO_2$ presence is often undesirable as it lowers the energy content of the natural gas and causes pipeline corrosion. The natural gas must be first processed for removal of impurities to meet the specifications of marketable natural gas and to avoid pipeline corrosion. A wide range of technologies including cryogenic distillation, absorption, adsorption, and membrane separation have been developed to separate $CO_2$ from natural gas, or more specifically $CO_2$ from $CH_4$ [1]. Among these technologies, membrane separation received wide attention as it is promising in gas purification process with attractive advantages besides being commercially viable [2].

Membrane-based technology has continuous growth and breakthroughs over the past decades and offer desirable features such as high energy efficiency, ease of control, environmental compatibility and low operating costs [3]. Membrane technology also supports fast and stable separation without any phase changes [4].

Despite the advantages of membrane technology such as low manufacturing costs and processing ability, it has some limitations that subsequently lead to development of inorganic membranes. The inorganic materials have preferable properties but it is difficult to duplicate in large scale due to high capital cost. Recently, the emergence of mixed matrix membranes (MMMs) is an innovative approach to incorporate the

advantages of both polymeric membrane and inorganic materials [5]. It is a new membrane technology that is made up of inorganic fillers dispersed evenly in a polymer membrane.

The emergence of MMM offers a solution to the trade-off upper bound of polymeric membranes [6], possessing possibly better chemical, mechanical and separation properties. The ideal filler in MMMs should possess good properties as a molecular sieve or gas adsorbent and excellent dispersion properties in the submicron-thick polymer matrix. It should also yield high quality interfaces with the polymer [7]. There are many types of inorganic fillers such as zeolites, carbon molecular sieves (CMS), metal oxides and silica [8].

In this study, MCM-41 (Mobil Composition of Matter No. 41), a mesoporous material with a hierarchical structure from a family of silicate and alumosilicate solids, is used as the inorganic filler in the MMM of Polysulfone (Psf) polymer. Psf is used as polymer-based as it is easy to process and commercially available. In facing the challenges of MMM fabrication (see Chapter 2.5), amine functionalized MCM-41 particles are incorporated in Psf membrane to enhance the MMM surface morphology and gas separation performance. The percentage loading of filler is set constant as 0.1 wt % and 1 wt%, as the optimum silica loading reported in Psf polymeric membrane is 0.1 wt% [9].

## 1.2 Problem statement

The performance of the membrane largely depends on the choice of membrane materials, characterized by its chemical, permeation and mechanical properties.  The key focus area in MMM is the development of a membrane that possess high selectivity and permeability, besides having good mechanical resistance to the separation process parameters and conditions. MMM has the excellent separation properties of molecular sieves combined with low lost and good processing of polymers. However in real structures of MMM, voids exist around the filler particles and the polymer matrix. The polymer chain is detached from the surface of the filler particles due to incompatibility of the two phases.

While modification of inorganic MCM-41 particles by adding primary amine groups can improve the filler dispersion in MMM [10, 11], the influence on MMM gas permeability remains disputable. As the grafting of primary amine groups is shown to decrease the interfacial voids present in unmodified MCM-41 particles and improve the morphology, the question on the effect of higher level of amine functionalization on MCM-41 has been raised. The incompatibility of MCM-41 filler and Psf polymer still exists while there is no study yet that uses higher levels of amine functionalization on MCM-41 in MMM fabrication. In an attempt to create well dispersed fillers in MMM with high permeability while maintaining the selectivity, the MCM-41 particles are further functionalized with secondary amine groups in this study, in addition to the primary amine-functionalized MCM-41 and original MCM-41 parent silica. The performance of the secondary amine-functionalized MCM-41 is evaluated and compared with the original MCM-41 and primary amine-functionalized MCM-41 through morphology and gas permeability study. A highly permeable and selective MMM structure free of defects and interfacial voids, as well as containing homogenously distributed filler particles, is desired for gas separation membranes.

A defect-free and void-free MMM with homogenous distribution of fillers exhibiting excellent separation properties is still a major challenge in the development of MMM. The novelty of the present study is the secondary amine functionalization on MCM-41 fillers embedded in Psf MMM, in comparison to primary amine functionalization of the fillers.

### 1.3 Objectives

1. To fabricate primary and secondary amine-functionalized MCM-41/Psf MMM.

2. To characterize the membrane using Transmission Electron Microscope (TEM), Scanning Electron Microscope (SEM), Fourier Transform Infrared Spectroscopy (FT-IR) and Energy-dispersive X-ray spectroscopy (EDX).

3. To study the performance of the amine-functionalized MCM-41/Psf MMM in $CO_2/CH_4$ separation.

## 1.4 Relevance and Feasibility

The key advance of MMM is to increase the gas permeability and selectivity, well above the trade-off upper limit by Robeson [6]. The two properties, permeability and selectivity often do not increase with each other. Hence, the synthesis of high permeability MMM while maintaining the selectivity is important in membrane technology. The performance of gas separation of $CO_2$ from $CH_4$ in natural gas will be improved. In addition, a better MMM which could overcome the limitations of the polymeric membrane and inorganic membrane could revolutionize the membrane technology.

The research project is feasible within the time frame to achieve its objective. It is shown clearly through the Gantt chart in Chapter 3.6.

# CHAPTER 2

# LITERATURE REVIEW AND THEORY

## 2. LITERATURE REVIEW AND THEORY

### 2.1 Polymeric Membrane

Recently, research has been focused on the separation of gases by polymeric membranes. This technology is dynamic and growing fast. Polymeric membranes were favored due to its reproducibility, excellent mechanical properties and cheap manufacturing cost. The mechanisms of gas transport depend on the solubility and diffusivity of the permeant molecules. The types of polymers that have been reported widely in the literature including, polysulfone (Psf), polyetherimide (PEI), polyimide (PI) and polyethersulfone (PESf) [4].
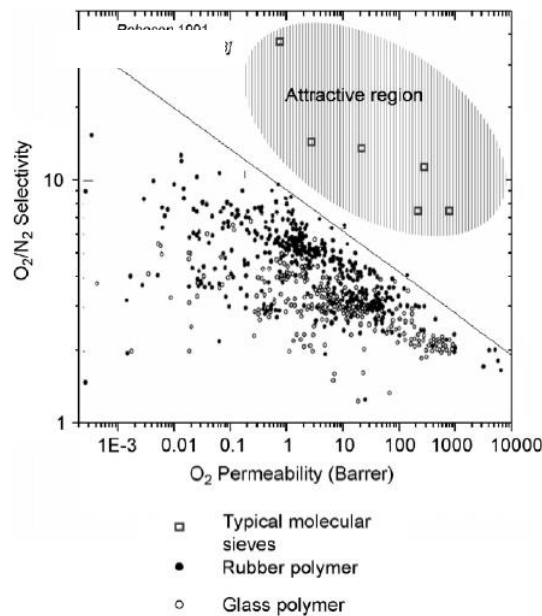


**Figure 1: Relationship between selectivity and permeability [6]**

Polymeric membranes were preticted by Robeson to have an upper limit in performance of gas separation [6]. A trade-off can be observed in Figure 1, and is referred to as the "upper bound" line. The other limitations by polymeric membranes are low selectivity, swelling, instability in high temperature and decomposition in organic solvents [12]. Despite many efforts have been made to improve the separation properties, it is still a challenge to increase the trade-off line by a huge difference. The increase of permeability was often at the expense of selectivity, and vice versa [9, 13, 14].

Despite the benefit of polymeric membranes including energy efficiency, usage of toxic-free chemical and ease of operation, it has several limitations. It suffers from thermal instability, poor chemical resistance, swelling and decomposition in organic solvents [13, 14]. In addition, polymeric membranes suffer from plasticization due to the effect of $CO_2$ at high pressure. Beyond the critical pressure, $CO_2$ causes swelling or dilation of membrane that leads to reduced selectivity and permeability [9].

Psf is one of the most widely explored polymers for $CO_2/CH_4$ separation [2, 9]. Figure 2 shows a Psf repeating unit. Psf is a type of glassy polymer that have a rigid and mechanically robust structure that gives better gas separation compared to rubbery polymers, which gives high flux but low selectivity. It also has high selectivity thanks to their strong size-sieving capability [15]. Psf is selected as the polymer membrane in the study due to its commercial value and ease of processing, as well as good mechanical properties and chemical stability [9]. However, it has poor mobility of polymer chains that leads to weak interaction between the polymer matrix and the inorganic fillers [2]. The inadequate wetting of the polymer causes the formation of interfacial voids, which will be discussed in the following section.
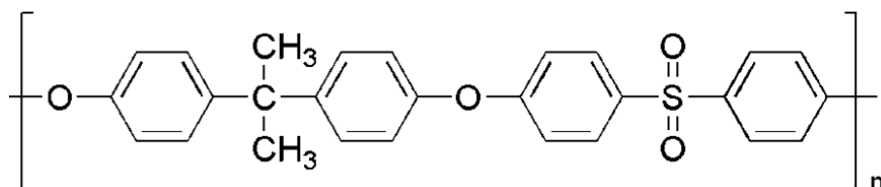


**Figure 2: Polysulfone repeating unit. [16]**

6

## 2.2 Inorganic Membrane

The limitations of polymeric membranes has led to the development of inorganic membrane and other althernative membrane materials. Inorganic membranes can withstand elevated temperature for a long duration and is durable to harsh separation enviromnent [4]. They also exhibit longer lifespans than polymeric membranes. Although some of the inorganic membranes have desirable properties above the trade-off line, their duplication and large-scale production is difficult, besides the expensive cost of raw materials of the inorganic materials [5]. The commercialization of inorganic membranes is difficult to be realised due to the cost. Moreover, inorganic membranes are bittle and have low surface-to-ratio volume [17]. Hence, research is underway to overcome the limitations by polymeric and inorganic membranes.

## 2.3 Concept of Mixed Matrix Membranes (MMMs)

In incorporating the advantages from both polymeric membranes and inorganic membranes together, the state of the art membrane technology, MMM, is introduced. Figure 3 shows MMM as a heterogeneous membrane having inorganic filler ingrained in a polymer matrix. MMM comprises of organic polymer (bulk phase A) and inorganic particles (dispersed phase B) as fillers, which may be zeolite, carbon molecular sieves, or other nano-sized as well as mesoporous particles. It is expected to have strong adhesiveness between organic and inorganic composite, enhanced separation performance and good mechanical properties [5].
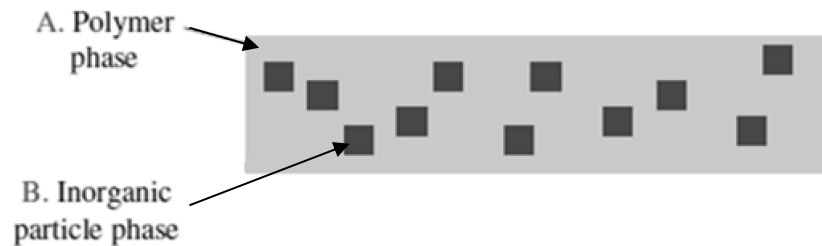


**Figure 3: Schematic of a MMM [18]**

MMMs can potentially achieve higher permeability, selectivity or both properties compared to the original polymeric membranes, due to the superior separation

characteristics of the inorganic particles. Additionally, the brittleness of the inorganic membranes is solved as flexible polymer is used as the continuous matrix [18]. Table 1 compares the advantages of each type of membrane. MMM are shown to be favorable in many aspects of membrane properties and performance, and it solves the problems of organic and inorganic membranes altogether.

**Table 1: Comparison of the properties for gas separation membranes [19]**

|  | Properties | Polymeric membrane | Inorganic membrane | MMM |
|---|---|---|---|---|
| i | Cost | Economical to fabricate | High fabrication cost | Moderate |
| ii | Chemical and thermal stability | Moderate | High | High |
| iii | Mechanical strength | Good | Poor | Excellent |
| iv | Compatibility to solvent | Limited | Wide range | Limited |
| v | Swelling | Frequent | None | None |
| vi | Separation performance | Moderate | Moderate | Robeson upper boundary |
| vii | Handling | Robust | Brittle | Robust |

Due to its enhanced gas separation properties, MMMs have the potential to enhance gas separation properties at high temperature and pressure. Different types of materials have been researched as fillers for this purpose [4, 14, 15]. However, formation of defect-free MMMs faces with many challenges. The challenges will be further discussed in Chapter 2.4.

An excellent MMM is defined by high permeability, selectivity, as well as good thermal and mechanical stability. The separation efficiency of MMM is predicted by Maxwell model [4, 14]. The $CO_2/CH_4$ gas separation performances of MMM reported in the literature are summarized in Table 2. From the table, different materials for the polymeric membrane have been tried for comparison, as well as inorganic fillers in varying loadings. It is shown that in most cases, the permeability of the MMM is in reverse relationship with selectivity when filler weightage increase. Finding the

optimum filler loading with desirable trade-off between permeability and selectivity is important. The loading percentage differs depending on the type of MMM compositions.

**Table 2: Advances of MMMs in $CO_2/CH_4$ gas separation**

| MMM Composition | | Pressure (atm) | Temperature (°C) | $CO_2$ permeability (Barrer) | Ideal selectivity, $\alpha_{CO2/CH4}$ | Reference |
|---|---|---|---|---|---|---|
| Polymer | Filler (Loading) | | | | | |
| Matrimid® PI | CMS (36 vol%) | - | - | 12.6 | 51.7 | [14, 20] |
| ABS | AC (62.4 vol%) | - | 5 | 6.67 | 50 | [14, 21] |
| ABS | AC (2 w/v) | - | 30 | 5.04 | 21.63 | [15, 22] |
| | AC (5 w/v) | | | 6.85 | 23.63 | |
| | AC (7 w/v) | | | 9.70 | 26.94 | |
| | AC (10 w/v) | | | 13.41 | 28.90 | |
| | AC (20 w/v) | | | 8.43 | 21.95 | |
| PES | A zeolite with silver ion exchange (50 wt %) | | | 1.2 | 44 | [14, 23] |
| Psf | MCM-48 (0 wt %) | 4 | 35 | 4.46 | 26.23 | [15, 24] |
| | MCM-48 (10 wt %) | | | 8.45 | 25.61 | |
| | MCM-48 (20 wt %) | | | 18.21 | 23.65 | |
| Psf | SWNT (0 wt %) | 4 | 35 | 3.90 | 22.94 | [15, 25] |
| | SWNT (5 wt %) | | | 5.12 | 18.96 | |
| | SWNT (10 wt %) | | | 5.19 | 18.53 | |
| | SWNT (15 wt %) | | | 4.52 | 16.14 | |
| Matrimid® | MOF-5 (0 wt %) | 2 | 36 | 9.00 | 41.70 | [15, 26] |
| | MOF-5 (10 wt %) | | | 11.10 | 53.63 | |
| | MOF-5 (20 wt %) | | | 13.80 | 40.59 | |
| | MOF-5 (30 wt %) | | | 20.20 | 44.89 | |
| Matrimid® | Meso-ZSM-5 (0 wt %) | - | - | 7.29 | 34.71 | [15, 27] |
| | Meso-ZSM-5 (10 wt %) | | | 8.27 | 67.19 | |
| | Meso-ZSM-5 (20 wt %) | | | 8.65 | 66.07 | |
| | Meso-ZSM-5 (30 wt %) | | | 14.61 | 56.48 | |
| Matrimid® | Cu-BPY-HFS (0 wt %) | - | 35 | 7.29 | 34.71 | [15, 28] |
| | Cu-BPY-HFS (10 wt %) | | | 7.81 | 31.93 | |

| | | | | | | |
|---|---|---|---|---|---|---|
| | Cu-BPY-HFS (20 wt %) | | | 9.88 | 27.62 | |
| | Cu-BPY-HFS (30 wt %) | | | 10.36 | 27.45 | |
| | Cu-BPY-HFS (40 wt%) | | | 15.06 | 25.55 | |
| Matrimid® | C60 (0 wt %) | - | | 7.15 | 36.00 | [15, 29] |
| | C60 (2.5 wt %) | | | 5.00 | 37.72 | |
| | C60 (5 wt %) | | | 4.54 | 35.75 | |
| | C60 (10 wt %) | | | 3.79 | 34.77 | |
| Matrimid® 5218 | CMS 800-2 (0 vol %) | 3.5 | 35 | 10.00 | 35.30 | [15, 20] |
| | CMS 800-2 (17 vol %) | | | 10.30 | 44.78 | |
| | CMS 800-2 (19 vol %) | | | 10.60 | 46.09 | |
| | CMS 800-2 (33 vol %) | | | 11.50 | 47.92 | |
| | CMS 800-2 (36 vol %) | | | 12.60 | 52.50 | |
| Ultem® 1000 | CMS 800-2 (0 vol %) | 3.5 | 35 | 1.45 | 43.00 | [15, 20] |
| | CMS 800-2 (16 vol %) | | | 2.51 | 43.26 | |
| | CMS 800-2 (20 vol %) | | | 2.90 | 48.33 | |
| | CMS 800-2 (35 vol %) | | | 4.48 | 53.98 | |
| PC | zeolite 4A (0 wt %) | - | 25 | 8.80 | 23.50 | [15, 30] |
| | zeolite 4A (20 wt %) | | | 7.80 | 32.50 | |
| | zeolite 4A (30 wt %) | | | 7.00 | 37.60 | |
| PC | zeolite 4A (0 wt %) | 3.65 | 25 | 8.80 | 23.53 | [15, 31] |
| | zeolite 4A (5 wt %) | | | 8.40 | 31.60 | |
| | zeolite 4A (10 wt %) | | | 8.20 | 32.80 | |
| | zeolite 4A (20 wt %) | | | 7.80 | 32.50 | |
| | zeolite 4A (30 wt %) | | | 7.0 | 37.60 | |
| PC | pNA (0 wt %) | 3.65 | 25 | 8.80 | 23.53 | [15, 31] |
| | pNA (1 wt %) | | | 4.20 | 40.38 | |
| | pNA (2 wt %) | | | 4.00 | 51.95 | |
| | pNA (5 wt %) | | | 3.90 | 53.42 | |
| Psf | $Cu_3(BTC)_2$ (0 wt %) | - | | 6.49 | 18.75 | [15, 32] |
| | $Cu_3(BTC)_2$ (10 wt %) | | | 3044 | 3.36 | |

| | | | | | |
|---|---|---|---|---|---|
| | Cu₃(BTC)₂ (20 wt %) | | | 2929 | 3.46 | |
| | $Cu_3(BTC)_2$ (30 wt %) | | | 2900 | 3.55 | |
| | $Cu_3(BTC)_2$ (40 wt %) | | | 2562 | 3.06 | |
| PDMS | $Cu_3(BTC)_2$ (0 wt %) | - | | 2502.47 | 3.13 | [15, 32] |
| | $Cu_3(BTC)_2$ (10 wt %) | | | 3046.99 | 3.31 | |
| | $Cu_3(BTC)_2$ (20 wt %) | | | 2927.01 | 3.45 | |
| | $Cu_3(BTC)_2$ (30 wt %) | | | 2898.93 | 3.63 | |
| | $Cu_3(BTC)_2$ (40 wt %) | | | 2559.81 | 3.04 | |
| Psf | $Mn(HCOO)_2$ (0 wt %) | - | | 6.49 | 18.75 | [15, 32] |
| | $Mn(HCOO)_2$ (5 wt %) | | | 6.45 | 14.75 | |
| | $Mn(HCOO)_2$ (10 wt %) | | | 6.83 | 9.16 | |
| PPZ | SAPO (22 wt %) | 3.57 | 22 | 48.00 | 17.50 | [15, 33] |
| Psf | Silica 0.00 (vf) | 4.4 | 35 | 6.30 | 28.64 | [15, 34] |
| | Silica 0.05 (vf) | | | 7.70 | 26.55 | |
| | Silica 0.10 (vf) | | | 9.30 | 24.47 | |
| | Silica 0.15 (vf) | | | 12.90 | 18.69 | |
| | Silica 0.20 (vf) | | | 19.70 | 17.91 | |
| PES | Zeolite beta (20 wt %) | 10 | 35 | 1.63 | 32.6 | [15, 35] |
| Ultem® | MFI crystals (0 wt %) | 2 | 35 | 1.40 | 38.00 | [15, 36] |
| | MFI crystals (20 wt %) | | | 2.20 | 43.00 | |
| | MFI crystals 3(0 wt %) | | | 2.00 | 45.00 | |
| Matrimid® | MFI crystals (0 wt %) | 2 | 35 | 76.00 | 35.00 | [15, 36] |
| | MFI crystals (35 wt %) | | | 31.00 | 39.00 | |
| PVAc | CuTPA (0 wt %) | - | - | 2.44 | 34.90 | [15, 37] |
| | CuTPA (15 wt %) | | | 3.26 | 40.40 | |
| PES | zeolite NaN (0 wt %) | 10 | 35 | 2.65 | 31.55 | [15, 38] |
| | zeolite NaN (20 wt %) | | | 1.44 | 28.33 | |
| | zeolite NaN (30 wt %) | | | 1.24 | 31.79 | |
| | zeolite NaN (40 wt %) | | | 1.05 | 35.35 | |
| PES | zeolite AgA (0 wt %) | 4.4 | 35 | 2.65 | 31.55 | [15, 38] |

| Polymer | Filler | | | CO₂ permeability (Barrer) | Ideal selectivity | Reference |
|---|---|---|---|---|---|---|
| | zeolite AgA (20 wt %) | | | 1.67 | 37.95 | |
| | zeolite AgA (30 wt %) | | | 1.50 | 48.39 | |
| | zeolite AgA (40 wt %) | | | 1.21 | 55.00 | |
| | zeolite AgA (50 wt %) | | | 1.05 | 58.33 | |
| Matrimid® | CAe (0 wt %) | - | 35 | 7.29 | 34.70 | [15, 39] |
| | CAe (10 wt %) | | | 7.98 | 47.80 | |
| | CAe (20 wt %) | | | 9.92 | 47.80 | |
| | CAe (30 wt %) | | | 13.34 | 45.10 | |
| PI | MCM-41 | 8 | 1.75 | 17.00 | 58.62 | [15, 40] |
| PI | HZS | 8 | 2.75 | 18.70 | 87.62 | [15, 41] |
| C | SBA-15 | 24 | 1 | 1410.00 | 97.00 | [15, 42] |
| C | MCM-48 | 24 | 1 | 2461.00 | 98.00 | [15, 42] |

Table 3 shows the different fillers used for Psf in the MMMs. Comparing the permeability and ideal selectivity, MCM-41 give highest permeability and ideal selectivity among the other fillers. It shows that MCM-41/Psf MMM is a promising combination that offers better performance in separation and holds the prospect of raising the Robeson upper trade-off line.

**Table 3: Psf MMMs with different fillers2**

| Polymer | Filler | Pressure (atm) | Temperature (°C) | CO₂ permeability (Barrer) | Ideal selectivity, $\alpha_{CO2/CH4}$ | Reference |
|---|---|---|---|---|---|---|
| Psf | HKUST-1 (16 wt %) | 1 | - | 8.80 | 16.20 | [15, 43] |
| Psf | S1C (16 wt %) | 1 | - | 9.60 | 20.80 | [15, 43] |
| Psf | ZIF-8 (16 wt %) | 1 | - | 12.10 | 19.10 | [15, 43] |
| Psf | HKUST-1 + S1C (16 wt %) | 1 | - | 8.90 | 22.40 | [15, 43] |
| Psf | ZIF-8 + S1C (16 wt %) | 1 | - | 8.60 | 19.10 | [15, 43] |
| Psf | MCM-41 (8 wt%) | 4.40 | 35 | 14.00 | 41.20 | [2, 15] |
| Psf | HZS (8 wt%) | 2.75 | 35 | 7.20 | 37.55 | [15, 41] |

## 2.4 Mesoporous MCM-41

Different combinations of inorganic fillers and polymeric membrane have been researched in various studies. Among the common inorganic fillers used in MMM are zeolites [23, 30, 31, 36, 38, 43], carbon molecular sieves [20], ordered mesoporous silica [2, 10, 24, 40, 42, 44, 45], nanoparticles silica [34, 44], and carbon nanotubes [25, 46]. The choice of mesoporous material rather than microporous enhances the filler-polymer interaction. Mesoporous materials are characterized by their large pores (2-50 nm) and one of the common ordered mesoporous silica used in MMM recently is MCM-41 [10]. The mesoporous silicas have better filler-polymer interaction than other molecular sieves, attributed to large surface areas with sufficient silanol groups to create hydrogen bonding with polymer chains [4]. Figure 4 shows the representative structure of mesoporous MCM-41.
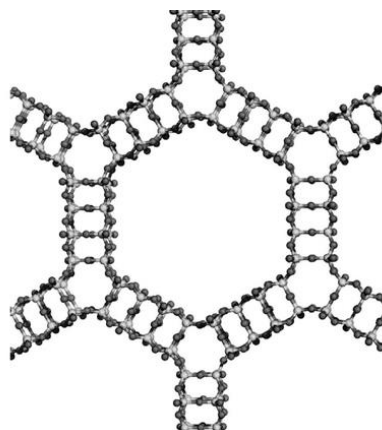


**Figure 4: Representative structure of MCM-41 mesoporous silica [47]**

A hexagonal member of mesoporous silica family, MCM-41 has a hierarchical one-dimensional pore structure. MCM-41 possesses good thermal stability and hydrothermal properties, and exhibit a vast amount of hydroxyl or silanol groups (~40-60%) for the ease of surface modification [48]. The study by Reid et al. [49] claims that mesoporous MCM-41 particles as inorganic fillers in MMM increase the MMM permeability while maintaining its selectivity as it is compatible with the polymer matrix. The pore diameter of mesoporous MCM-41 allows the Psf chain to penetrate into the filler porosity, which gives way to the establishment of intimate composites [2]. The rate of gas diffusivity is also faster in using MCM-41 compared to zeolites due to the high diffusivity tunnels and polymer chain redistribution at pore

entrance [4]. In addition to the separation of gas in polymer matrix via solution diffusion model, inorganic fillers assist the gas transport using molecular sieving mechanism [15]. The mechanism works by separating the molecules based on differences in their molecular size. Figure 5 shows the gas transport through filler in MMM.
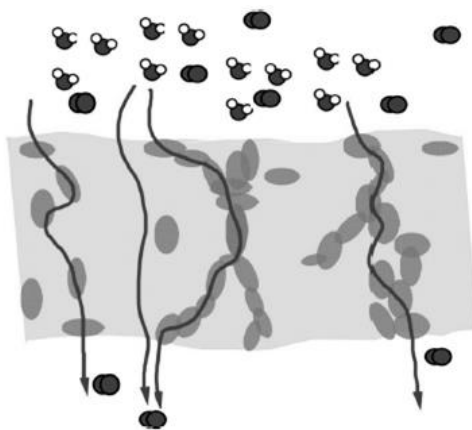


**Figure 5: Gas permeation through fillers in MMM [15]**

The loading amount of inorganic fillers in MMM is vital to achieve good gas separation performance. In the study by Kim et al. [44] that uses MCM-41 nanoparticles and Psf membrane, the ideal selectivity of $CO_2/CH_4$ before and after incorporation of MCM-41 up to 40 wt% is the same. However, the permeability of MCM-41/psf MMM increased significantly compared to pure Psf membrane.

The study by Zornoza et al. [2] shows that the selectivity decreased when the filler loading is high. It is attributed to the existence of defects in the MMM. This may be due to the overloading of filler that causes interfacial voids in the structure, thereby forming irregular pores that decrease the selectivity. The optimum loading in the study of Zornoza et al. is 8 wt % and its relationship between selectivity and permeability was located in the Robeson upper bound region.

**2.5 Challenges in Mixed Matrix Membrane Fabrication**

The main challenges faced in the process of fabricating the MMM are the control of the chemical structure as well as surface morphology, and the selection of inorganic filler which will affect the performance of the MMM. Particle agglomeration was observed during the preparation of MMM, making the solution preparation complicated as the agglomerates have to be broken up before fabrication.

In certain MMMs, the inorganic fillers used and the polymeric membrane are not fully compatible due to different physical properties and densities. Weak interactions between the filler particles and the polymer will create separate filler phases or layers during MMM formation [4]. It also resulted in the formation of interfacial voids between the filler particles and the polymer matrix. It often results in the increase of MMM permeability while decreasing its selectivity undesirably [50]. The formation of non-selective voids allows gas molecules bypass, shown in Figure 6a. In Figure 6b and 6c, to eliminate the interfacial voids, bridging agents were used in order to improve the surface interaction [4].
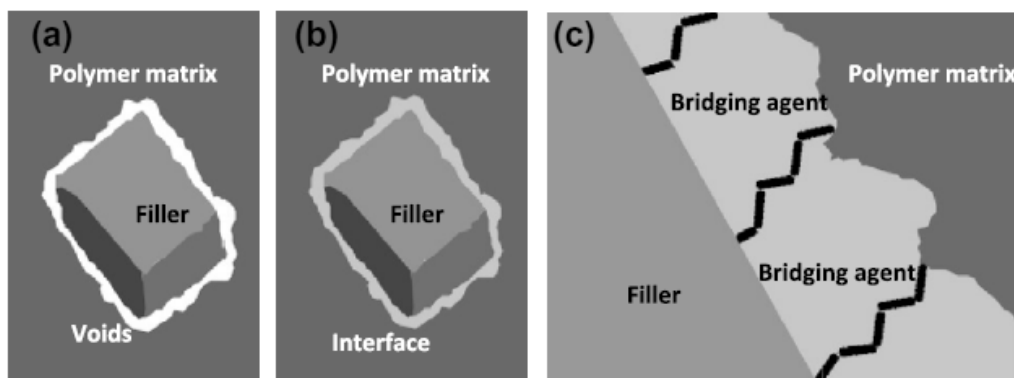


**Figure 6: Interphase properties of MMMs [4]**

In addition, the polymer in direct contact with inorganic filler is possible to become rigidified where the attached polymer chains become immobilized compared to those in polymer matrix. The rigidification often reduces the gas permeability while increase selectivity [14].

Another challenge is the filler pore blockage by the polymer chain. The partial or total blockage on the pores will impede the function of the filler particles, eventually reducing the permeability [4, 14, 50]. Figure 7 summarizes the ideal morphology (Case 1) and three interface morphology problems (Case 2-4) present in MMMs [14]. The focus area of the present study is mitigation of interfacial voids (Case 2). The void formation problem is most commonly encountered in MMM fabrication problems.
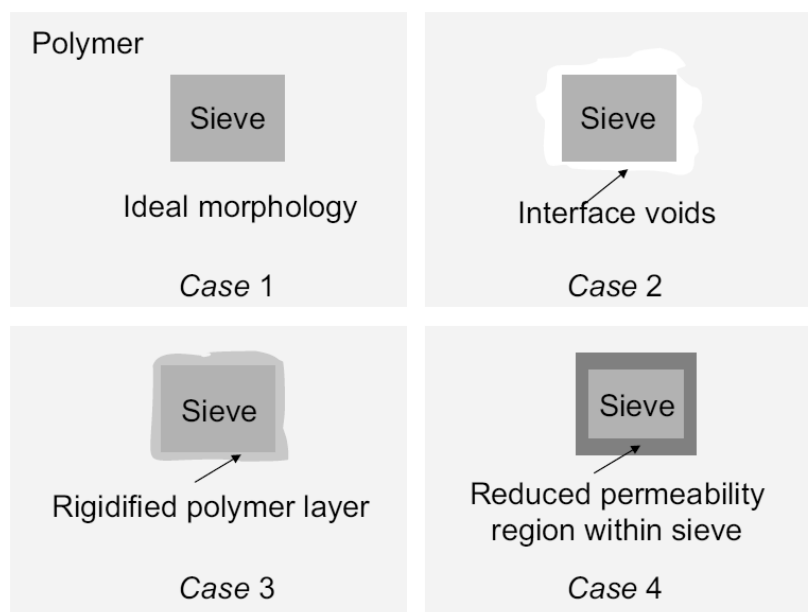
**Figure 7: The schematic diagram of different MMM morphology challenges [14]**

## 2.6 Optimization of Interface Morphology

The interface quality of the inorganic filler and polymer matrix is a very important aspect influencing the success of MMM. The key factor is the affinity between the two component in the MMM structure [4, 44].

The two main challenges in fabrication of Psf MMM are inorganic filler agglomeration and the incompatibility between the Psf and MCM-41 particles. These two problems will lead to the reduction of selectivity of the MMM. The first problem can be minimized by finding the optimum filler composition in Psf matrix. The second problem could be improved by changing the filler pore sizing, modifying the surface of filler and functionalizing the filler particles with bridging agents [9].

The heterogeneous MCM-41/Psf MMM can be optimized by controlling the filler in terms its loading and spatial dispersion. It can be achieved by silylation of organoalkoxysilane with surface silanol groups on the mesopores of the prefabricated mesoporous silica. It utilizes silanol group of mesoporous silicates as anchoring sites to graft organic functional groups. The reported organoalkoxysilanes used on mesoporous silica nanoparticles are 3-aminopropyltrimethoxysilane (APTMS), N-(2-aminoethyl)-3- aminopropyltrimethoxysilane (AAPTMS), 3-[2-(2-aminoethylamino)ethylamino]propyltrimethoxysilane (AEPTMS), ureidopropyltrimethoxysilane (UDPTMS), 3-isocyanatopropyltriethoxysilane

(ICPTES), 3-cyanopropyltriethoxysilane (CPTES), and allyltrimethoxysilane (ALTMS) [51]. The new hybrid organic–inorganic mesoporous ordered silica has functionalized pore channels of large diameter and high surface area that allows chemical interaction of surface groups and the functionalized pore channels [52].

To improve the dispersions of the filler in the membrane matrix, Kim et al. [44] modified the nano-sized MCM-41 particles by depositing primary amine functional groups. For the amine functionalization, 3-aminepropyltriethoxysilane (APTES) was used to form covalent bond of Si-O-Si with SiOH groups at the surface of silica. The amine functionalized MCM-41 gave better dispersion and increase in selectivity, compared to the unmodified MCM-41. The permeability, however, is less than unmodified MCM-41. Kim et al. also used the same procedure on MCM-48 particles [53]. Figure 8 shows the structure of APTES containing an amine group.
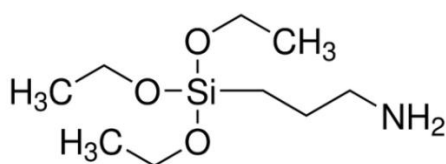


**Figure 8: Structure of ATPES [54]**

Another example of ATPES functionalization of amine group on mesoporous MCM-41 is shown by Mello et al. [11] to investigate the performance on $CO_2$ adsorption on MCM-41 alone without MMM. The bonds of amino groups to mesoporous silica are covalent bonds and the functionalization was claimed to have no effect on the MCM-41 hexagonal structure. The impregnation of amine on MCM-41 by reduced the pore sizes of the silica as they were blocked by aminopropyl groups. MCM-41-$NH_2$ was found to have better $CO_2$ sorption than MCM-41 at low pressure only [11]. The amount of amino groups attached to MCM-41 was found to have effect on the interaction mechanism between the structure and $CO_2$. Figure 9 shows the attachment of amine group to the surface of MCM-41.
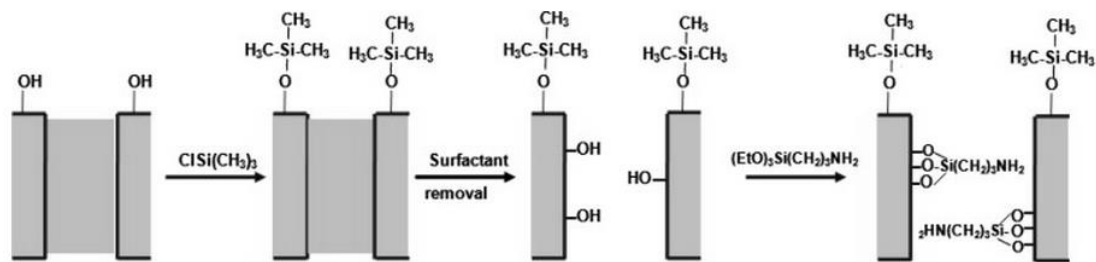
**Figure 9: Attachment of APTES to the surface of mesoporous MCM-41 [44]**

Khan et al. [10] have also synthesized amine-functionalized mesoporous MCM-41 covalently bonded to acrylate modified Psf MMM in an attempt to reduce interfacial voids. The fillers are modified by grafting (3-Aminopropyl)trimethoxysilane (APTMS). The resultant MMM was compared to unmodified MCM-41 MMM and it is found that the interfacial voids were greatly reduced (Figure 10). However, the modified MCM-41 have reduced pore sizes and it decreased the gas permeability compared to unmodified MCM-41, also observed by Mello et al [10, 11].
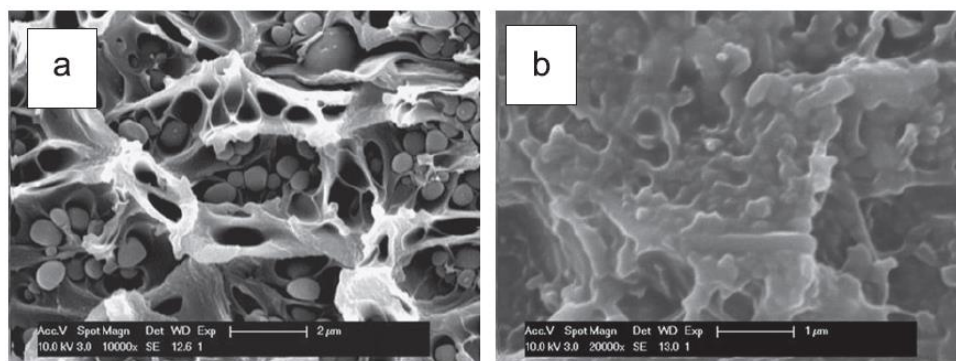


**Figure 10: The voids in unmodified MCM-41 (a) were almost eliminated in modified MCM-41 (b) [10]**

Amino functional groups were set on the surface of the prepared MCM-41 particles by using grafting method [10]. The secondary and tertiary amine-functionalization on MCM-41 in the study followed the same procedure, with AAPTMS (Figure 12) in replacement of APTMS respectively. Figure 13 shows the mechanism of amine-functionalization on MCM-41 by grafting method, using APTMS as the primary silane coupling agent.
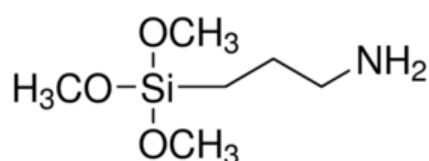


**Figure 11:  Structure of APTMS [55]**
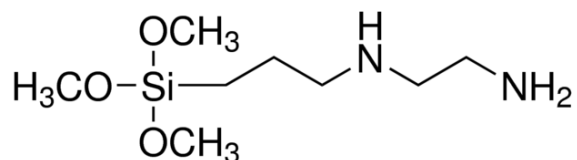
**Figure 12: Structure of AAPTMS [56]**
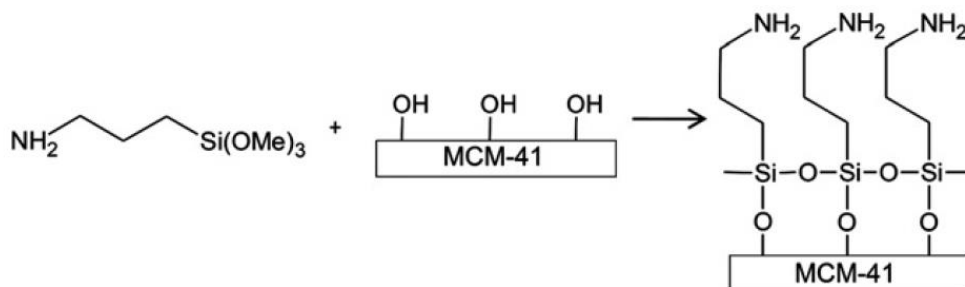


**Figure 13: Reaction of APTMS functionalization of MCM-41[10]**

In short, amine functionalization on inorganic fillers will alter surface morphology, improve two-phase compatibility and affect the gas separation properties of MMM. In the literature so far, there is no studies that graft secondary and tertiary amine groups on MCM-41 mesoporous particles. The effects of higher level amine functionalization of MCM-41 on MMM surface morphology, compatibility of the two phases, as well as permeability and selectivity are investigated in the study.

# CHAPTER 3

# METHODOLOGY

## 3. METHODOLOGY

### 3.1 Flowchart of the Overall Research Methodology

The overall research methodology is shown in Figure 14.

Synthesis of MCM-41 and amine-functionalization of mesoporous MCM-41

Synthesis of amine-functionalized MCM-41/Psf MMM

Characterization of MMMs

Gas permeability test

Results and discussion

Report writing
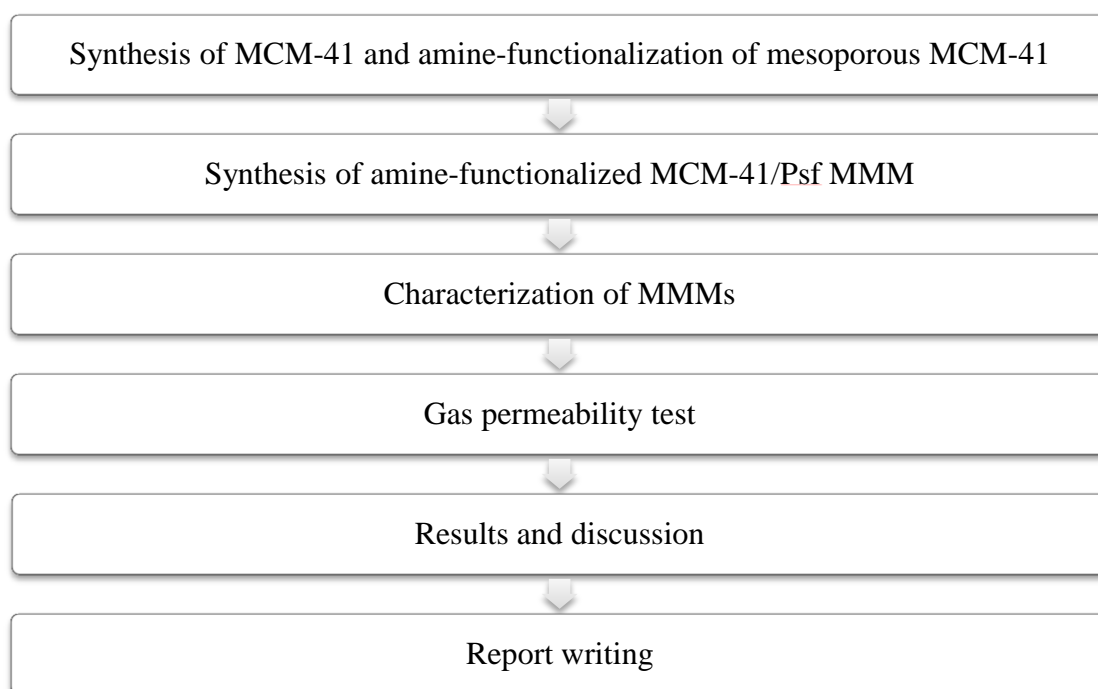
**Figure 14: Flow chart of the overall research methodology**

### 3.2 Materials

Membrane:

- Psf pellets, dried overnight
- N-Methyl-2-pyrrolidone (NMP) mixed with prescribed weightages

MCM-41:

- NaOH
- Dry toluene
- Cetyl trimethylammonium bromide (CTAB)
- Tetraethyl orthosilicate (TEOS)

Two types of functionalized MCM-41 inorganic fillers were synthesized from the MCM-41 parent silica:

a) Primary amine-functionalized MCM-41 (grafted using, APTMS)
b) Secondary amine-functionalized MCM-41 (grafted using AAPTMS)

### 3.3 Research Procedures

The method selected in synthesizing Psf-based MMM is the dry/wet process to obtain an asymmetric Psf polymeric membrane. An asymmetric membrane consists of two layers: a thin dense layer, and beneath it a highly porous and thick sublayer [57]. The dense layer is responsible for the permeability and selectivity of the MMM, while the sublayer only acts as mechanical support of the membrane structure, having minimal role on the gas separation. Hence, in the case of asymmetric membrane, the mass transfer and properties of the gas separation depends on the thickness of the dense layer instead of the entire membrane thickness [57]. Figure 15 shows the schematic cross-section of asymmetric membrane.
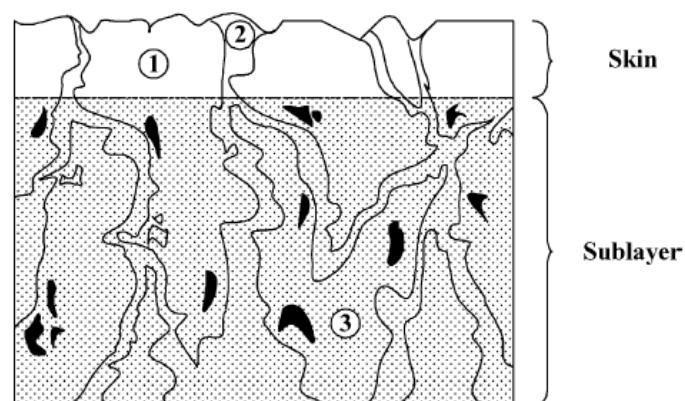


**Figure 15: Schematic representation of asymmetric membrane. Note: (1) Permeable dense layer (2) Pore (3) Highly porous sublayer [57]**

The main stages in dry/wet process includes polymer solution casting, convective and free-standing evaporation and subsequent immersion of the membrane in coagulation bath [9, 57]. The force evaporation step is done prior to bath immersion

to concentrate the outer layer of the membrane. The solvent exchange with methanol is carried out to minimize water surface tension in membrane pores. In the present study, the MMMs were prepared following the procedure published elsewhere [10, 44, 58].

### 3.3.1 Synthesis of MCM-41

1. 2M of NaOH solution was prepared by mixing 0.4 g NaOH in a 50 mL volumetric flask.
2. 480 ml of DI water, 3.5 ml of 2M NaOH and 1 g of CTAB were mixed in a polypropylene bottle.
3. The solution was stirred at 200 rpm and heated at 80°C for 30 min in a water bath. The bottle cap was closed.
4. When the mixture turned clear, 5 ml of TEOS was added into the solution. The reaction was continued for another 2 hours.
5. The solution was centrifuged (8000rpm) for 15 min to collect the suspended powders. Two visible layers were formed at the end of centrifugation.
6. The powders were washed with deionized (DI) water and centrifuged again for three times (8000rpm) for 5 min each. It was repeated with ethanol with the same settings.
7. The powders were collected in a petri dish and dried overnight in oven at 100°C to remove the moisture.
8. The powders were transferred into a crucible. Calcination was done at 500°C for 10 hours to remove the CTAB template in the MCM-41 particles.

### 3.3.2 Functionalization of MCM-41

1. 0.6 g of MCM-41 was mixed with 100 ml of dry toluene.
2. The mixture was stirred and heated up to 85°C for 30 min.
3. It was transferred into a round-bottom flask and 0.6 ml of APTMS was added.
4. The reaction was continued under reflux at 110 °C for 16 hours.
5. The resulting primary amino-functionalized MCM-41 was collected by centrifugation (8000 rpm) for 15 min.

6. The powders were washed with DI water and centrifuged again for three times (8000rpm) for 5 min each.

7. The collected particles were dried in petri dish at room temperature.

8. The steps were repeated for secondary amine-functionalized MCM-41 with AAPTMS respectively in replacement of APTMS.

### 3.3.3 Pure Psf Membrane Preparation

Phase inversion method by Junaidi et al. [58] is used to synthesise pure Psf membrane. The volume needed for each membrane casting is approximately 12 mL. Table 4 shows the calculation of Psf and NMP components to form the membrane.

1. Before preparation of membrane, psf pellets were dried overnight at 60°C to eliminate excess moisture.

2. (3.25 g) 25 wt% of Psf and (9.484 mL) 75 wt% NMP were prepared.

3. The Psf pellets were added into NMP solution and mixed at surrounding temperature for 12 h (500 rpm).

4. The polymer solution was sonicated for 4 h and left standing for a day to remove the trapped micro-bubbles.

5. The polymer solution was poured onto a clean glass plate and casted with a 0.025 mm gap casting knife at ambient temperature to create a flat sheet layer membrane.

6. A force evaporation step of 30 s was allowed for the growth of thin dense layer.

7. The flat layered solution was submerged in DI water bath for 24 h.

8. The fabricated membrane was solvent-exchanged with MeOH for 2 h, and air-dried for 5 minutes, and moved to the desiccator for 3 days.

**Table 4: Volume for pure Psf membrane**

| Chemical | wt% | Density (g/mL) | Mass (g) | Volume (mL) | Membrane volume (mL) | Membrane mass (g) |
|----------|-------|-------|--------|--------|--------|--------|
| PSf | 25.00 | 1.240 | 3.250 | 2.621 | 12.105 | 13.000 |
| NMP | 75.00 | 1.028 | 9.750 | 9.484 | | |

### 3.3.4 Fabrication of Psf and MCM-41 MMM

1. The required 0.1 wt% of MCM-41 particles was stirred in NMP solution for 2 h.
2. The solution was sonicated for 30 min.
3. 10 wt% of the overall required Psf (90 wt %) was added to the solution and mixed for 4 h. Sonication was continued for 30 min.
4. The remaining Psf solution was added and stirred again for a day.
5. The solution was again sonicated for 1 h to make sure the particles are dispersed homogeneously and to remove trapped micro-bubbles.
6. The polymer solution was poured onto a clean glass plate and casted with a 0.025 mm gap casting knife at ambient temperature to create a flat sheet layer membrane.
7. A force evaporation step of 30 s was allowed for the growth of thin dense layer.
8. The flat layered solution was submerged in DI water bath for 24 h.
9. The fabricated membrane was solvent-exchanged with MeOH for 2 h, and air-dried for 5 minutes, and moved to the desiccator for 3 days.

### 3.3.5 Characterization of MMMs

The characterization of the resultant membranes was done using a Fourier Transform Infrared (FT-IR) spectrometer to check the presence of surface functional groups attached to the MCM-41 in the MMM. The structural property of the MCM-41 before and after amine modification will be observed.

The morphology and dense layer thickness of the MMM is obtained using a Scanning Electron Microscope (SEM). Cross sectional view and plan view of the membrane will be done using SEM from the range of $1000 - 10000$ magnification [10, 58].

The structures of MCM-41 and amine-functionalized MCM-41 particles were observed using Transmission Electron Microscope (TEM). The average pore size and particle size of MCM-41, APTMS-MCM-41 and AAPTMS-MCM-41 were measured on the TEM images.

Energy dispersive X-ray (EDX) is conducted along with SEM to analyse the elemental composition of MCM-41 particles in the MMMs.

### 3.3.6 Gas Permeation Performance Test

The gas permeation performance test was done for the resultant membranes using permeation test rig. The apparatus set up is shown in Figure 16.
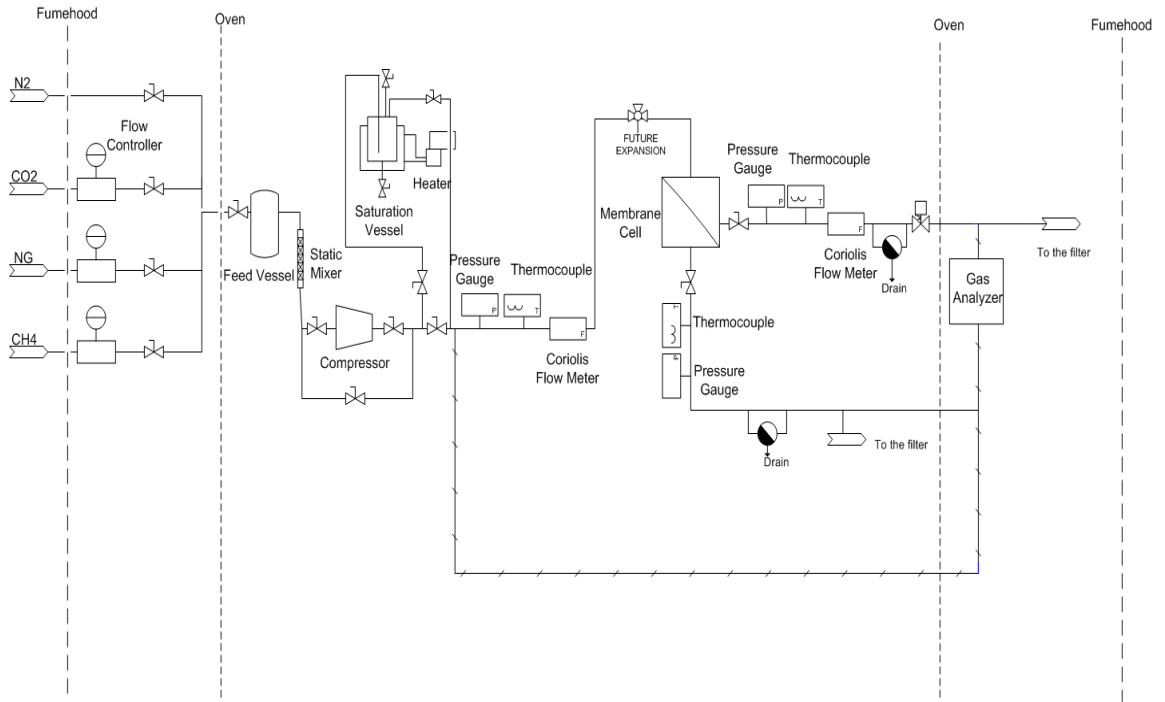


**Figure 16: Permeation test rig**

The permeability for pure gases was then calculated using equation (1) by Ismail and Lai [57]. The test was carried out with constant pressure method with feed pressure of 4 bar at room temperature [58]. A bubble flow meter is used to measure the volumetric flow rate of the permeate gas at atmospheric pressure.

$$\left(\frac{P}{l}\right)_i = \frac{Q_i}{A\Delta p} \tag{1}$$

Where

P is the the permeability of membrane

Q is the volumetric flow rate of gas

$\Delta p$ is the pressure difference across membrane

A is the membrane effective surface area

l is the membrane thickness

The permeability of the membrane is calculated using the permeate flow rate obtained from the bubble flowmeter and the pressure drop. The unit used in permeability of membranes is GPU. (GPU=$1\times10^{-6}$ cm$^3$ (STP)/cm$^2$s cm Hg). The $CO_2/CH_4$ ideal selectivity is calculated using Equation 2. $CO_2$ gas permeation is always conducted after $CH_4$ to minimize membrane plasticization by $CO_2$.

$$\alpha_{CO_2}/_{CH_4} = \frac{(P/l)_{CO_2}}{(P/l)_{CH_4}} \tag{2}$$

### 3.4 Project Activities & Key Milestones

The main project activities are synthesis of MCM-41 mesoporous particles, functionalization of MCM-41 particles, synthesis of pristine Psf membrane and MCM-41/Psf MMM, as well as characterization of the resulting membranes. The time needed for synthesis until recovery for each project activity is shown in Table 5.

Inorganic filler mesoporous MCM-41 is synthesized prior to the fabrication of MMM. The MCM-41 is modified with primary and secondary amine functional groups (APTMS and AAPTMS respectively). Then, MCM-41 and modified MCM-41 were doped in the Psf solution and mixed, then casted and fabricated to form MMMs. Four analytical apparatus (FT-IR, TEM, SEM and EDX) are used to characterize the MMMs.

**Table 5: Time for synthesis or recovery of membrane and particles**

| Synthesis of MCM-41 | | Functionalization of MCM-41 | | Synthesis of pure Psf membrane | | Fabrication of Psf and MCM-41 MMM | |
|---|---|---|---|---|---|---|---|
| Preparation | 6 | Preparation | 1 | Preparation | 1 | Preparation | 2 |
| Calcination | 10 | Reflux | 16 | Mixing | 10 | Sonication | 0.5 |
| | | Collection | 2 | Sonication | 4 | Mixing | 4 |
| | | | | Leave solution | 24 | Sonication | 0.5 |
| | | | | Casting | 1 | Mixing | 24 |
| | | | | Water bath | 12 | Sonication | 1 |
| | | | | Solvent exchange | 2 | Casting | 1 |
| | | | | Drying | 24 | Water bath | 12 |
| | | | | | | Solvent exchange | 2 |
| | | | | | | Drying | 24 |
| Total hour | 16 | Total hour | 19 | Total hour | 78 | Total hour | 71 |
| day | 2 | day | 3 | day | 5 | day | 4 |

Then, the performance of the resultant MMM in $CO_2/CH_4$ gas separation was tested using permeation test rig. The key milestones of the project are shown in Table 6.

**Table 6: Key milestones of the research**

| Milestone | Date of completion |
|---|---|
| Confirmation of title and supervision | 3/9/2014 |
| Preparation of synthesis procedures, literature review, etc. | 24/10/2014 |
| Synthesis of MCM-41 and amine-functionalized MCM-41 | 15/1/2015 |
| Fabrication of MMM | 27/2/2015 |
| Performance of gas permeation test | 20/3/2015 |
| Characterization of MMM (TEM, EDX, FESEM, FT-IR) | 31/3/2015 |

## 3.5 Equipment

Table 7 describes the purposes of the equipment used in the present study. Table 8 summarizes the chemical, glassware, equipment and characterization equipment and their details used in the study.

**Table 7: Purposes of the equipment used in the study**

| Equipment | Purposes |
|---|---|
| Sonicator | To disperse filler in the membrane and to remove the trapped air bubbles (degas) in the solution |
| Oven | To dry the polymer. |
| Casting knife | To cast the membrane |
| Centrifuge | To recover MCM-41 particles from particles solution |
| Furnace | To remove CTAB templates in calcination of MCM-41 |
| Scanning Electron Microscope (SEM) | To study the morphology and dense layer thickness of the MMM. |
| Transmission Electron Microscope (TEM) | To study the structure of MCM-41 and functionalized MCM-41 filler |
| Energy dispersive X-ray (EDX) | To check the element composition and confirm dispersion of inorganic fillers in MMM |
| Fourier transform infrared spectrophotometer (FT-IR) | To confirm the presence of inorganic fillers in the MMM and the structure of amine functionalized MCM-41 |
| Permeation test rig | To test the performance of the membrane in $CO_2/CH_4$ gas separation. |

**Table 8: Chemical, glassware and equipment list**

| Type | No. | Name | Amount | Manufacturer | Location (rack) |
|---|---|---|---|---|---|
| Chemical | 1 | Psf | 3.36 g | Sigma Aldrich | 05-00-01 |
| | 2 | NMP | 9.972 g | Merck | 05-00-01 |
| | 3 | MeOH | | Merck | 05-00-01 |
| | 4 | NaOH | 0.6729 g | EMSURE | 05-00-01 |
| | 5 | Toluene | 300 ml | Merck | 05-00-01 |
| | 6 | CTAB | 3 g | Merck | 05-00-01 |
| | 7 | TEOS | 15 ml | Merck | 05-00-01 |
| | 8 | APTMS | 1.8 ml | Sigma Aldrich | 05-00-01 |
| | 9 | AAPTMS | 1.8 ml | Sigma Aldrich | 05-00-01 |
| Glassware | 1 | Reflux unit | x 1 | - | 05-00-01 |
| | 2 | Measuring cylinder | 250 ml, 10 ml | - | 05-00-01 |
| | 3 | Beaker | 500 ml | - | 05-00-01 |
| | 4 | Centrifuge tubes | 6 | - | 05-00-01 |
| | 5 | Glass plate | 3 | - | 05-00-01 |
| | 6 | Polypropylene bottle | 1 | - | 05-00-01 |
| | 7 | Petri dish | 1 | - | 05-00-01 |
| | 8 | Round bottom flask | 1 | - | 05-00-01 |
| | 9 | Crucible | 1 | - | 05-00-01 |
| | 10 | Magnetic stirrer | 1 | - | 05-00-01 |
| Equipment | 1 | Electronic balance | 1 | - | 05-00-01 |
| | 2 | Hotplate magnetic stirrer | 1 | - | 05-00-01 |
| | 3 | Oven | 1 | Binder | 05-01-03 |
| | 4 | Sonicator | 1 | Fisherbrand | 03-02-03 |
| | 5 | Casting knife | 1 | OEM | 05-00-01 |
| | 6 | Centrifuge | - | Heraeus | 05-01-03 |
| | 7 | Furnace | - | Protherm | 05-01-03 |
| Characterization equipment | 1 | SEM | - | - | 17-00-03 |
| | 2 | EDX | - | - | 04-02-09 |
| | 3 | FT-IR | - | - | 04-02-13 |
| | 4 | TEM | | - | Block P |
| | 5 | Gas Permeation Test Rig | - | - | 05-00-01 |

## 3.6 Gantt Chart

Table 9 shows the planning and Gantt chart for the present research work. The green boxes are for submission milestones.

**Table 9: Gantt chart for FYP I and II**

| Project Activities | FYP I Sept 1 | 2 | Oct 3 | 4 | 5 | 6 | Nov 7 | 8 | 9 | 10 | Dec 11 | 12 | 13 | 14 | 15 (Study week) | 16 (Exam week) | FYP II Jan 1 | 2 | 3 | Feb 4 | 5 | 6 | 7 | Mar 8 | 9 | 10 | 11 | Apr 12 | 13 | 14 | 15 |
|---|---|---|---|---|---|---|---|---|---|---|---|---|---|---|---|---|---|---|---|---|---|---|---|---|---|---|---|---|---|---|---|
| Confirmation of supervision and title | Y | Y | | | | | | | | | | | | | | | | | | | | | | | | | | | | | |
| Preliminary research work | | | Y | Y | Y | Y | Y | | | | | | | | | | | | | | | | | | | | | | | | |
| Submission of extended proposal | | | | | | | G | | | | | | | | | | | | | | | | | | | | | | | | |
| Proposal defense | | | | | | | | Y | | | | | | | | | | | | | | | | | | | | | | | |
| Synthesis of MCM-41 | | | | | | | | | Y | Y | | | | | | | | | | | | | | | | | | | | | |
| Amine-functionalized MCM-41 | | | | | | | | | | | Y | Y | Y | | | | | | | | | | | | | | | | | | |
| Submission of interim report | | | | | | | | | | | | | G | | | | | | | | | | | | | | | | | | |
| Synthesis of pure Psf membrane | | | | | | | | | | | | | | Y | | | Y | | | | | | | | | | | | | | |
| MMM fabrication | | | | | | | | | | | | | | | | | | Y | Y | Y | Y | | | | | | | | | | |
| Submission of progress report | | | | | | | | | | | | | | | | | | | | | | | G | | | | | | | | |
| MMM characterization | | | | | | | | | | | | | | | | | | | | | Y | Y | Y | Y | | | | | | | |
| Pre-SEDEX | | | | | | | | | | | | | | | | | | | | | | | | | G | | | | | | |
| Permeability testing | | | | | | | | | | | | | | | | | | | | | | | | | Y | Y | Y | | | | |
| Submission of dissertation | | | | | | | | | | | | | | | | | | | | | | | | | | | | G | | | |
| Submission of technical paper | | | | | | | | | | | | | | | | | | | | | | | | | | | | G | | | |
| Viva | | | | | | | | | | | | | | | | | | | | | | | | | | | | | G | | G |
| Submission of hardbound dissertation | | | | | | | | | | | | | | | | | | | | | | | | | | | | | | | G |

30

# CHAPTER 4

# RESULTS AND DISCUSSION

## 4. RESULTS AND DISCUSSION

### 4.1 Characterization of MCM-41 and Amine-functionalized MCM-41 particles

Mesoporous silica MCM-41 was successfully synthesized and the particles were characterized using TEM and FT-IR. Figure 17 shows the TEM images of the MCM-41, APTMS-MCM-41 and AAPTMS-MCM-41 particles obtained in the present work. As illustrated in Figure 17, all particles show highly ordered with uniform pores of hexagonal shape, which is comparable with those results reported in the literature [44]. Referring to Figure 17(b) and 17(c), the MCM-41 representative hexagonal pore arrangement was maintained after amine functionalization.

Figure 18 shows the particle distribution of MCM-41 and amine-functionalized MCM-41 particles in the TEM images. The MCM-41 particles agglomerated and formed clusters of particles. On the other hand, APTMS-MCM-41 and AAPTMS-MCM-41 particles show dispersed arrangement with reduced agglomeration compared to MCM-41, illustrating the repellence behavior of amino-propyl (APTMS) and amino-ethyl-amino-propyl groups (AAPTMS). The silanol groups on the surface of MCM-41 silica are hydrophilic [59]. The repellence of amine-functionalized MCM-41 is mainly due to the change of hydrophilic MCM-41 surface to hydrophobic surface after the amine functional groups are grafted on the surface of MCM-41, since the amine functional groups are hydrophobic in nature [51]. The interaction between silica particles is reduced, hence minimizing the formation of irregular MCM-41 agglomeration.

The MCM-41 particles in Figure 18 have particle diameter of 100±30 nm. Table 10 states the average particle sizes of the particles measured from the TEM images. The

particle sizes are comparable to the reported values from literature [10, 59]. MCM-41 silica is shown to have good reproducibility and stable towards amine functionalization.
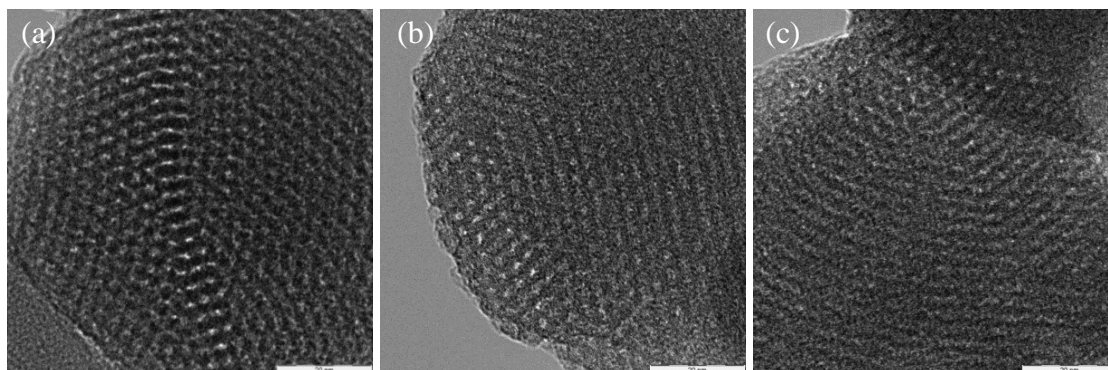


**Figure 17: Hexagonal structure of (a) MCM-41 (b) APTMS-MCM-41 (c) AAPTMS-MCM-41**
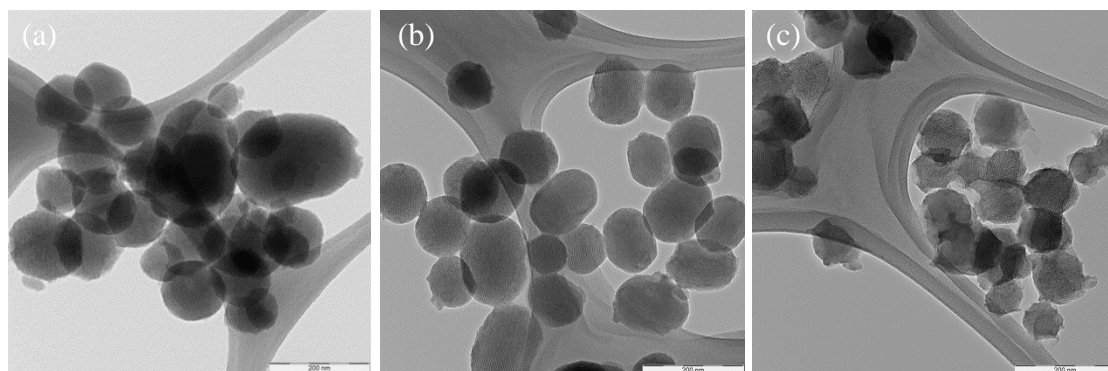


**Figure 18: Agglomeration observation of particles on wire gauze (a) MCM-41 (b) APTMS-MCM-41 (c) AAPTMS-MCM-41**

**Table 10: Structural properties of MCM-41 particles**

| Property | MCM-41 | APTMS-MCM-41 | AAPTMS-MCM-41 |
|---|---|---|---|
| Average particle size (nm) | 108.14 | 102.99 | 94.44 |

Figure 19 shows the FT-IR spectra for the resultant fillers. Referring to Figure 19, MCM-41, APTMS-MCM-41 and AAPTMS-MCM-41 particles exhibit similar features of organic containing silica material. The fingerprint region of MCM-41 is at the FT-IR

peaks in the wavelengths range of 1235-1240 cm$^{-1}$ [60], and  1080–1090cm$^{-1}$ [61], due to the Si-O asymmetric stretching band in the Si-O-Si structure. Another characteristic of MCM-41 is the peak at ~968 cm$^{-1}$ and this peak is only present in the unmodified MCM-41, due to Si-O- (Si-OH) stretch present on the surface of the particle [48]. The peak from 1630–1640 cm$^{-1}$ is attributed to the absorption for H-O-H bending vibration in water [48, 61]. The band at around ~795 cm$^{-1}$ is contributed by the symmetric stretching of Si-O in Si-O-Si [48]. The broad band around 3100-3700 cm$^{-1}$ is a cause of –OH bonding from adsorbed water molecules [48, 61].

The completion of functionalization of amino groups by primary (APTMS) and secondary (AAPTMS) silane coupling agents was confirmed by the N-H bending vibration at ~690 cm$^{-1}$ [60, 61], and NH$_2$ symmetric bending vibration at ~1530cm$^{-1}$ [61]. For APTMS-MCM-41 and AAPTMS-MCM-41, the Si-OH vibration band at ~968 cm$^{-1}$ is absent as compared to MCM-41 [48, 61]. This is mainly due to the interaction between the silanol groups and –NH$_2$ groups, which may lead to Si-O-N$^+$H$_2$R or Si-O-N$^+$HR formation [60, 61].

The peak at ~2930cm$^{-1}$ corresponds to the n-CH and d-CH vibrations of the surfactant molecules due to incomplete calcination [61]. It is suggested to heat the samples at 550 °C to completely remove the surfactant templates.  The remaining template could block the pores of MCM-41 and hinders the penetration of polymer into the filler structure [2].
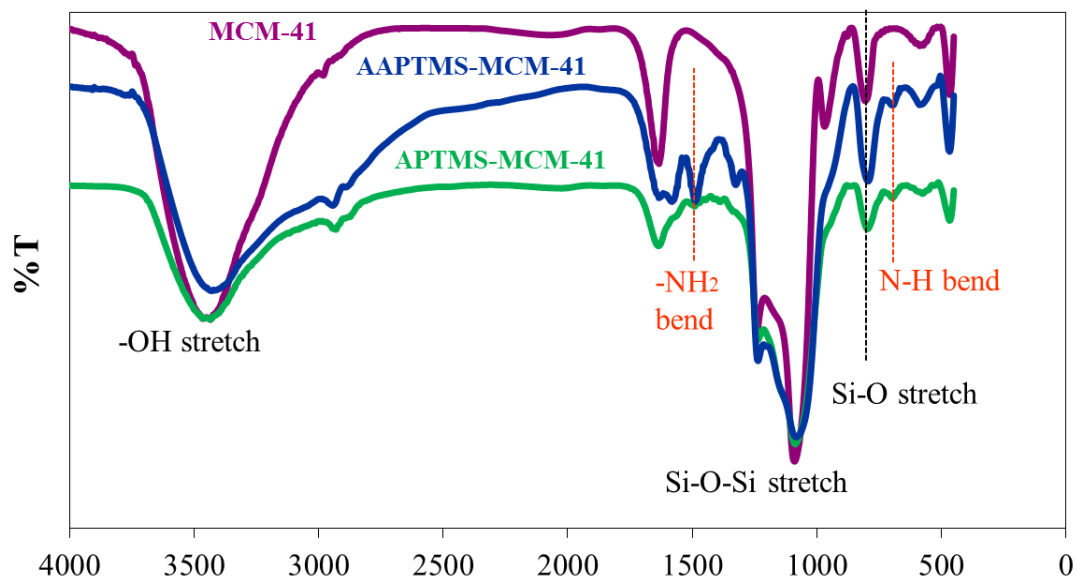
**Figure 19: FT-IR spectra of MCM-41, APTMS-MCM-41 and AAPTMS-MCM-41**

## 4.2 Morphology of Mixed Matrix Membranes (MMMs)

The cross-sectional and surface morphologies of MCM-41/Psf MMMs were observed using SEM. Figure 20 shows MMM cross sectional view loaded with 0.1 wt% and 1 wt% MCM-41, APTMS-MCM-41 and AAPTMS-MCM-41, respectively. It can be observed that there is a thin dense layer supported by porous substructure beneath the dense layer. The two distinct layers show that MMM is an asymmetric membrane and the thin dense layers of the MMMs are about 2μm thick measured from the SEM cross sectional images.

Agglomeration of particles were found on the MMMs loaded with 1 wt% particles , as shown in the cross-sectional SEM micrographs (Figure 20). The white clusters of agglomerates in 1wt% loaded MMM were more compared to 0.1 wt% loaded MMM for all types of filler (MCM-41 and amine-functionalized MCM-41). These results show that at higher loading, MCM-41 particles tend to clustered together more easily due to the weak filler-polymer matrix interaction. Albeit agglomerations of filler particles were inevitable, the agglomerations were reduced by functionalization of the filler in a way that the amine groups help to reduce filler-filler interaction.

| | 0.1 wt% | 1 wt% |
|---|---|---|
| (a) | | |
| (b) | | |
| (c) | | |
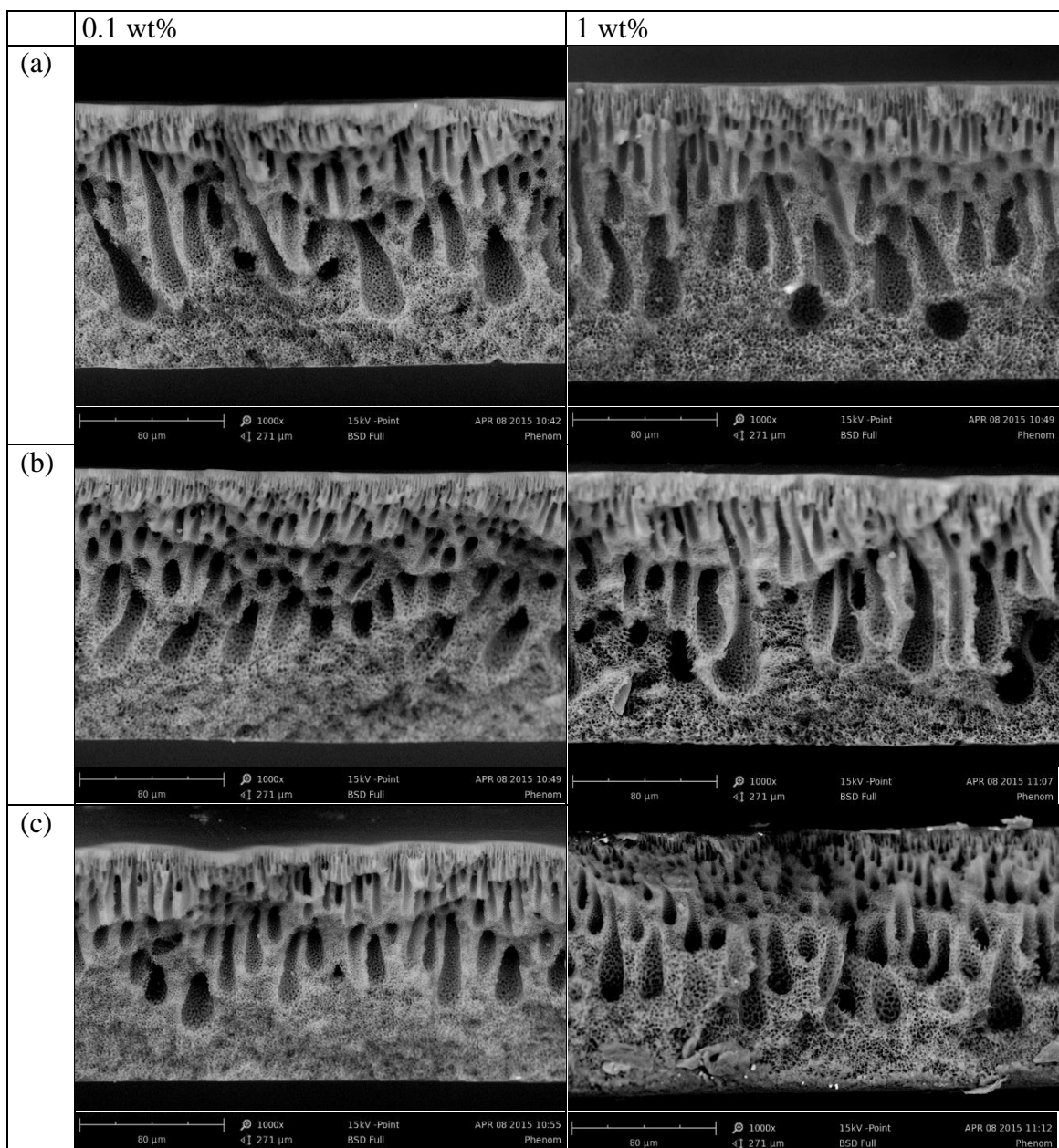
**Figure 20: SEM micrographs of MMM cross-section view (a) MCM-41/Psf (b) APTMS-MCM-41/Psf (c) AAPTMS-MCM-41/Psf**

Figure 21 shows the top-surface view of SEM micrographs for MMM loaded with 0.1 wt% particles. A porous structure is visible within the polymer matrix. From Figure 22, MMM loaded with 1 wt% of MCM-41 shows irregular agglomerates formed on the surface of the membrane, where it altered the surface structure of the dense layer by causing unselective void formations.
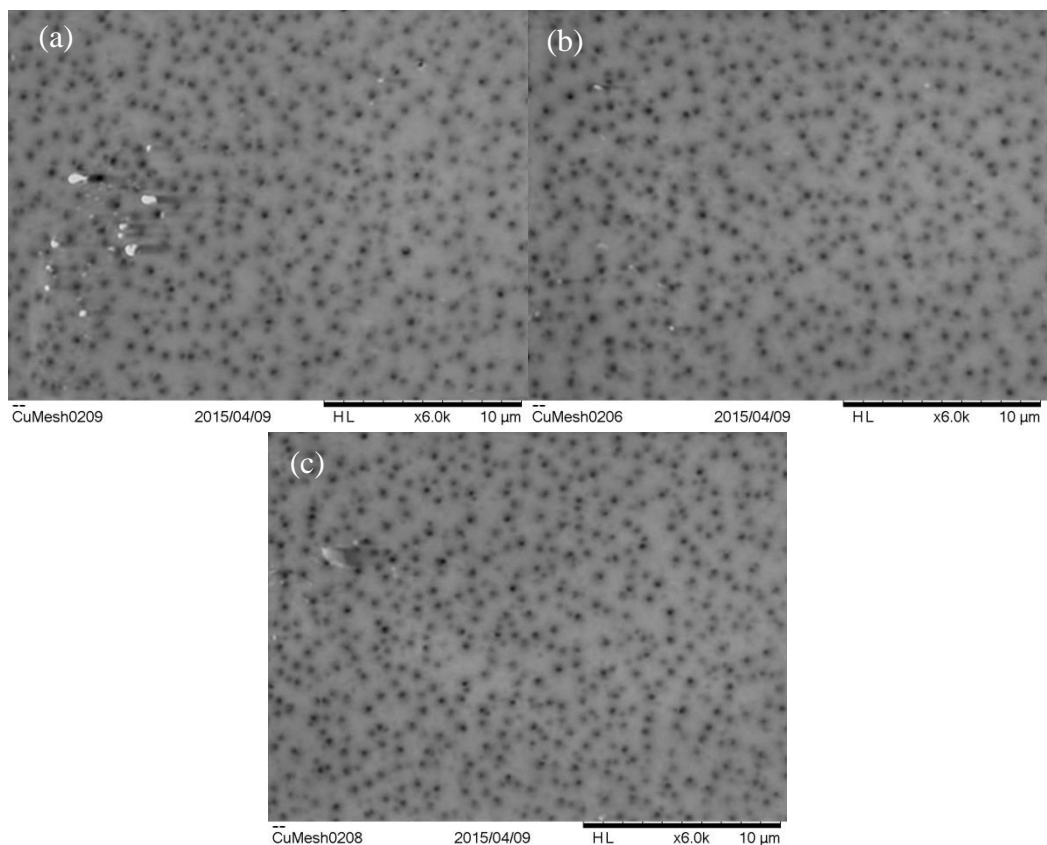
**Figure 21: Top surface view of SEM micrographs for MMM loaded with 0.1 wt% of particles (a) MCM-41/Psf (b) APTMS-MCM-41/PSf (c) AAPTMS-MCM-41/Psf**
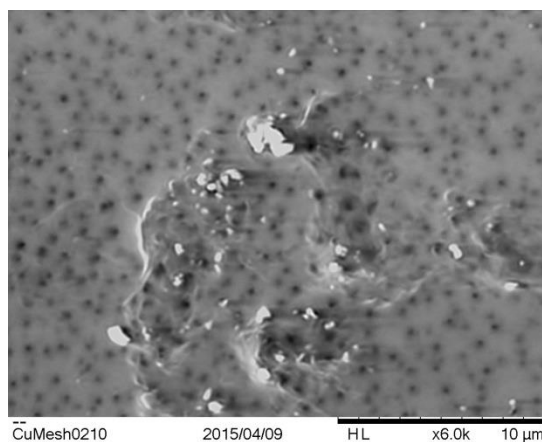


**Figure 22: Agglomeration of MCM-41 particles on 1 wt% MCM-41/Psf MMM**

The surfaces of the MMMs shown in Figure 21 were analyzed using EDX and the elemental composition in atomic percent is presented in Table 11. For APTMS-MCM-41 and AAPTMS-MCM-41, nitrogen element is present due to the attachment of amino

propyl groups on the particles, further confirmed the successful grafting of amines group on MCM-41.

**Table 11: Analysis of C, O, S, Si and N elements in MMM**

| Atomic content | MCM-41 | | APTMS-MCM-41 | | AAPTMS-MCM-41 | |
|---|---|---|---|---|---|---|
| (at %) | 0.1 wt % | 1 wt % | 0.1 wt % | 1 wt % | 0.1 wt % | 1 wt % |
| C | 83.03 | 72.48 | 78.52 | 74.34 | 78.89 | 73.16 |
| O | 14.53 | 22.31 | 14.34 | 17.92 | 14.15 | 19.23 |
| S | 2.40 | 2.50 | 2.31 | 2.59 | 2.30 | 2.61 |
| Si | 0.04 | 1.70 | 0.02 | 1.09 | 0.03 | 1.56 |
| N | - | - | 5.12 | 4.05 | 4.62 | 3.44 |

## 4.3 Gas Permeation Performance Testing

Single gas permeation tests of $CH_4$ and $CO_2$ were conducted for all synthesized membranes. The volumetric flow rate through the bubble flowmeter was measured for at least four times and the average value was taken for calculation of permeability. Table 12 shows the $CO_2$ and $CH_4$ gas permeation data of pure Psf membrane and MMMs, and Table 13 shows the percentage increase of permeance taking pure Psf membrane as a basis for comparison.

Referring to Table 13, the permeance of $CO_2$ and $CH_4$ gases increased significantly after addition of MCM-41 filler into Psf polymer matrix. The general trend is that the permeance for both gases increases with filler loadings for MCM-41, APTMS-MCM-41 and AAPTMS-MCM-41. For MMM loaded with 0.1 wt% fillers, APTMS-MCM-41/Psf demonstrated the highest permeance compared to MCM-41/Psf and APTMS-MCM-41/Psf. Percentage increment of 410.44% was obtained for $CO_2$ permeance, followed by MCM-41/Psf with percentage increment of 114.10%. AAPTMS-MCM-41/Psf shows a decrease in permeance, possibly due to thicker dense layer formed compared to the other MMM loaded with 0.1% of particles. It can also be a result of pore blockage by the long chain of amino-ethyl-amino-propyl groups present in AAPTMS-MCM-41 particles. For the MMM loaded with 1wt% particles, APTMS-MCM-41/Psf maintains its highest permeance with the percentage increment of 569.97%, followed by AAPTMS-MCM-41/Psf (309.32%) and MCM-41/Psf (182.61%).

The increase in permeance of the MMMs was accompanied by a drop in ideal selectivity, $\alpha(CO_2/CH_4)$. Referring to Table 12, the loss of selectivity from the MMMs might be due to several aforementioned reasons, i.e. morphology defects and dense layer thickness. Filler agglomerations on the surface observed on Figure 22 could be the primary cause of Psf matrix in having a lower affinity to $CO_2$ gas, leading to reduced selectivity of the MMM [58]. The arrangement of the polymer matrix in the dense layer of membrane is disrupted, resulting in unselective voids that allow gas bypass, explaining the increase in permeance and the loss of selectivity.

Taking the MCM-41/Psf MMM as reference, the functionalization of MCM-41 maintained the selectivity while increased the permeance for 0.1 wt% and 1 wt% loaded MMM, as shown in Table 12. Higher permeance obtained in functionalized MCM-41/Psf compared to MCM-41/Psf can be explained by enhanced interaction between filler and polymer matrix and reduced agglomerations of fillers due to the amine groups. This helps in generating a well-dispersed heterogeneous solution for the synthesis of MMM. From the current trend, primary amine functionalization using APTMS has a better overall performance than secondary amine functionalization using AAPTMS in terms of permeance for both 0.1 wt% and 1 wt% loaded MMM. AAPTMS has an extra amino-ethyl group added to the end of the common amino-propyl group exhibited by both silane coupling agents. The extra functional group could possibly alter the particle structural properties of the functionalized MCM-41 particles. Different organic functional groups have an effect on the morphology of mesoporous silica particles [51], thus influencing the interfacial interactions between the fillers and polymer matrix.

Based on the gas separation data, an increase of permeability always come with decreased selectivity, showing that the gas separation performance of MMMs follows the Robeson's trade-off bound. The inverse relationship between permeability and selectivity is observed. Figure 23 shows the performance of $CO_2/CH_4$ performance of the membranes prepared in this work in the Robeson's plot. Referring to Figure 23, the performance of the MMMs was below the trade-off boundary due to different methods of filler preparation and membrane fabrication. The calculation of the conversion of $CO_2$ permeability unit from GPU to Barrer is shown in Table 14 in Appendix I.

**Table 12: $CO_2$ and $CH_4$ gas permeation data of pure Psf membrane and MMMs**

| Loading | | Permeance (GPU) | | Ideal selectivity |
|---|---|---|---|---|
| % (w/w) | Type of fillers | $CO_2$ | $CH_4$ | $\alpha(CO_2/CH_4)$ |
| 0 | - | 35.53 | 29.86 | 1.19 |
| 0.1 | MCM-41 | 76.07 | 105.79 | 0.72 |
| | APTMS-MCM-41 | 181.36 | 246.85 | 0.73 |
| | AAPTMS-MCM-41 | 21.94 | 15.80 | 1.39 |
| 1 | MCM-41 | 100.41 | 161.09 | 0.62 |
| | APTMS-MCM-41 | 238.04 | 348.85 | 0.68 |
| | AAPTMS-MCM-41 | 145.43 | 226.70 | 0.64 |

**Table 13: Performance of Pure Psf and MMMs**

| Loading | | Permeance difference (%) | | Ideal selectivity |
|---|---|---|---|---|
| % (w/w) | Type of fillers | $CO_2$ | $CH_4$ | difference (%) |
| 0 | - | 0 | 0 | 0 |
| 0.1 | MCM-41 | 114.10 | 254.29 | -39.50 |
| | APTMS-MCM-41 | 410.44 | 726.69 | -38.66 |
| | AAPTMS-MCM-41 | -38.25 | -47.09 | 16.81 |
| 1 | MCM-41 | 182.61 | 439.48 | -47.90 |
| | APTMS-MCM-41 | 569.97 | 1068.29 | -42.86 |
| | AAPTMS-MCM-41 | 309.32 | 659.21 | -46.22 |
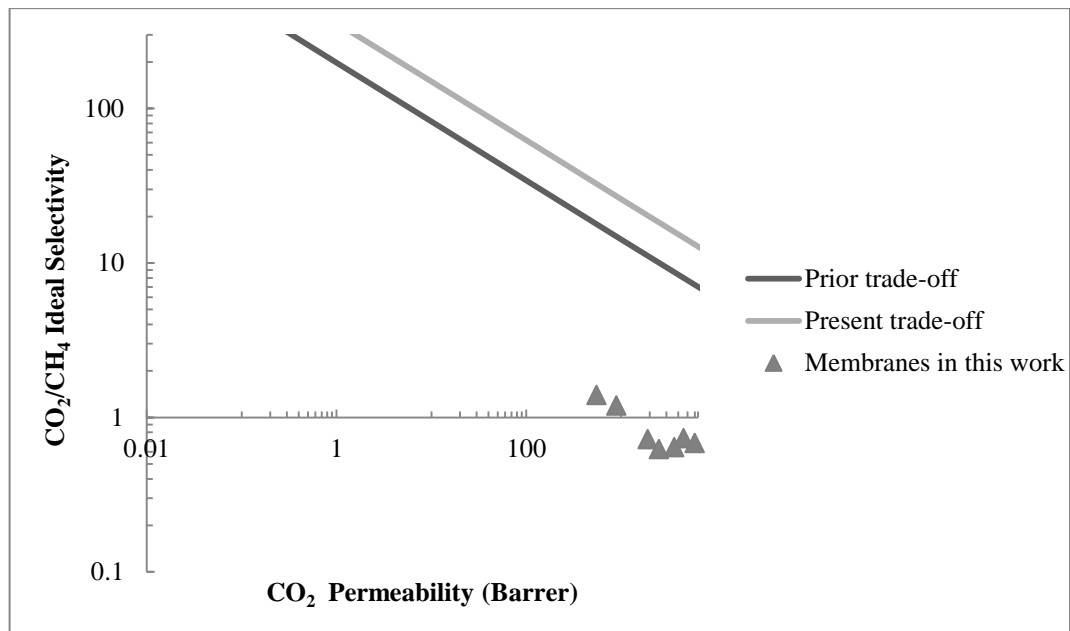


**Figure 23: Performance of MMMs based on Robeson's plot**

For pure Psf membrane, the gas permeation for both test gases is higher than the values reported in the literature [62], however with reduced selectivity. As permeability is largely attributed to the dense layer thickness, the much higher permeability values obtained in the permeation test suggested that the thickness of the MMMs is too low to give effective selectivity for $CO_2/CH_4$ gas separation. It may also be due to the abundance of defects on the membrane, or that the voids formed were more than threshold limit.

Due to different processing of polymer preparation and modification in MMM fabrication procedure, the selectivity values for MCM-41/Psf MMM are lower while permeance were much higher compared to the values reported in literature review [14, 59, 63]. It is noted that, however, the MCM-41/Psf MMM formulation and fabrication procedure in this work is slightly different than the fabrication of MMM reported in the literature. There are various parameters and aspects in membrane formulation that have substantial effect on the performance on the MMM, apart from morphology defects such as voids or particles agglomeration. The variables include the ratio of solvent, shear rate during manual casting, ambient humidity level, methods of placing membrane in the water bath, condition of solvent evaporation, sonication time and intervals, and other conditions of MMM solution preparation [9]. There were several other issues that may contribute to the difference in gas separation performance, some observed during the fabrication of MMM. During the immersion of MMMs in the deionized water bath, wrinkles were formed on the surface of MMM, which contributes to the defects in the morphology. Besides, the presence of bubbles in the MMM solution prior to casting also cause voids formation on the MMM, leading to a loss of selectivity. The bubbles were formed during MMM solution stirring and sonication period. The higher permeability of MMMs was also attributed to force evaporation time which influences thickness of the thin dense layer. Shorter force evaporation time prior to bath immersion produces thinner dense layer hence increased permeability.

# CHAPTER 5

# CONCLUSION & RECOMMENDATION

## 5. CONCLUSION AND RECOMMENDATION

### 5.1 Conclusion

The primary challenges faced in MMM fabrication are the control of the chemical structure as well as surface morphology, which greatly influence the performance of the MMM. The incompatibility of the organic filler and polymer matrix causes particle agglomeration during the preparation of MMM, as well as separate filler phases or layers during MMM formation due to the weak interaction of the two phases. In the case of MCM-41 and Psf membrane, undesirable interfacial voids are present in the MMM surface, decreasing the selectivity of the MMM. The increase of permeability is at the expense of selectivity, and vice versa.

MCM-41 silica is selected as filler in the MMM as it possesses good thermal stability and hydrothermal properties, besides having abundance of silanol groups for the ease of surface modification [48]. MCM-41 silica particles have been functionalized with amino propyl silane agents to improve its physical and chemical properties on the parent silica. As primary amine functionalization could help to improve the surface morphology of MMM, MCM-41 is grafted secondary silane agent AAPTMS in the study, in addition to the primary amine group using APTMS. MCM-41/Psf MMMs are synthesized using dry-wet method with 0.1 wt% and 1 wt% filler loadings.

The particle sizes of APTMS and AAPTMS functionalized MCM-41 fillers are 100±30 nm from TEM images. The TEM images also show that the hexagonal structure of MCM-41 remained intact after functionalization FT-IR spectra confirmed the successful

grafting of the organosilane groups on MCM-41. This suggests that grafting process is a viable method to modify mesoporous silica without loss of structural order. Cross sectional and surface views of MMM were obtained using SEM, and the elemental analysis was done on MMM surface using EDX. Amine functionalization on MCM-41 is effective in reducing the agglomeration of fillers, besides promoting the distribution of particles in polymer matrix.

MCM-41/Psf MMM permeability is increased after functionalization of MCM-41. In comparing between the two types of functionalization silane agents, APTMS has a better performance than AAPTMS in terms of permeance, while both maintain the selectivity of MCM-41/Psf MMM. Having an extra amino-ethyl group to the end amino-propyl group, the particle morphology of MCM-41 was possibly modified by AAPTMS. Hence, the interfacial interactions between the fillers and polymer matrix were also affected. Generally, the permeability of the MMMs increases with filler loadings for MCM-41, APTMS-MCM-41 and AAPTMS-MCM-41. However, increased permeability comes with loss of selectivity, indicating that MMM gas separation is still limited by Robeson's trade-off bound. The contradictory relationship of permeability and selectivity remains one of the limitations in the production of asymmetric MMM.

## 5.2 Recommendation

As the key challenges in the study are to minimized void formation and reduce particle agglomeration, synthesis of a defect-free MMM helps to raise the Robeson trade-off bound of selectivity and permeability. While the surface morphology of the MMM is substantial in affecting the gas separation performance, the thickness of the dense layer is vital to ensure good MMM separation properties. The membrane preparation procedure should be revised to find the effective membrane thickness for MCM-41/Psf MMM. Particle agglomeration can be reduced if a mechanical grinder or sieve is used instead of manual grinding of particles in mortar. Besides, the filler loading on MCM-41/Psf MMM can be varied to determine the optimum loading in Psf matrix.

For future work, 3-[2-(2-aminoethylamino)ethylamino]propyltrimethoxysilane (AEPTMS) can be grafted on MCM-41 silica to compare the gas separation

42

performance of the MCM-41/Psf MMM. In the literature so far, there is no studies that modify MCM-41 with AEPTMS to be used in Psf MMM. The effects of higher level amine functionalization of MCM-41 on particle morphology, MMM surface morphology as well as its permeability and selectivity are yet to be investigated.

Other than MCM-41 silica, primary (APTMS), secondary (AAPTMS) and tertiary (AEPTMS) silane agents can be grafted on MCM-48 mesoporous silica, a relative of MCM-41. MCM-48 has a regular three-dimensional channel network, move favorable compared to only one-dimensional pores of MCM-41. It also provides better mass transfer kinetics than the latter. Due to its structure, MCM-48 is less susceptible to pore blockage of amine groups, and a faster diffusion can be anticipated [64]. It may give higher permeability and better gas separation performance than MCM-41.

.

# REFERENCES

[1]     O. G. Nik, "Novel Functionalized Fillers For Mixed Matrix Membranes For $CO_2/CH_4$ Separation," PhD, Department Of Chemical Engineering Laval University Quebec, 2012.

[2]     B. Zornoza, S. Irusta, C. Téllez, and J. Coronas, "Mesoporous silica sphere-polysulfone mixed matrix membranes for gas separation," *Langmuir,* vol. 25, pp. 5903-5909, 2009.

[3]     A. L. Khan, C. Klayso, A. G. , and I. F. J. Vankelecom, "Polysulfone acrylate membranes containing functionalized mesoporous MCM-41 for CO2 separation," *Journal of Membrane Science,* pp. 145-153, 2013.

[4]     P. S. Goh, A. F. Ismail, S. M. Sanip, B. C. Ng, and M. Aziz, "Recent advances of inorganic fillers in mixed matrix membrane for gas separation," *Separation and Purification Technology,* vol. 81, pp. 243-264, 10/10/ 2011.

[5]     A. L. Ahmad, Z. A. Jawad, S. C. Low, and S. H. S. Zein, "Prospect of Mixed Matrix Membrane towards CO2 Separation," *Journal of Membrane Science and Technology,* vol. 2, p. 110, 2012.

[6]     L. M. Robeson, "Correlation of separation factor versus permeability for polymeric membranes," *Journal of Membrane Science,* vol. 62, pp. 165-185, 10/1/ 1991.

[7]     S. Kim, "High Permeability/High Diffusivity Mixed Matrix Membranes For Gas Separations," ed. Blacksburg, VA, 2007.

[8]     Y. Zhang, J. Sunarso, S. Liu, and r. wang, "Current status and development of membranes for CO2/CH4 separation: A review," *International Journal of Greenhouse Gas Control,* p. International Journal of Greenhouse Gas Control, 2013.

[9]     I. G. W. Helen Julian, "Polysulfone membranes for CO2/CH4 separation: State of the art," *IOSR Journal of Engineering,* vol. 2, pp. 484-495, 2012.

[10]    A. L. Khan, C. Klaysom, A. Gahlaut, and I. F. J. Vankelecom, "Polysulfone acrylate membranes containing functionalized mesoporous MCM-41 for CO2 separation," *Journal of Membrane Science,* vol. 436, pp. 145-153, 6/1/ 2013.

[11]  M. R. Mello, D. Phanon, G. Q. Silveira, P. L. Llewellyn, and C. M. Ronconi, "Amine-modified MCM-41 mesoporous silica for carbon dioxide capture," *Microporous and Mesoporous Materials,* vol. 143, pp. 174-179, 8// 2011.

[12]  A. B. Shelekhin, E. J. Grosgogeat, and S.-T. Hwang, "Gas separation properties of a new polymer/inorganic composite membrane," *Journal of Membrane Science,* vol. 66, pp. 129–141, 1992.

[13]  A. L. J. Ahmad, Z. A.; Low, S. C.; Zein, S. H. S., "Prospect of Mixed Matrix Membrane towards $CO_2$ Separation," *Journal of Membrane Science and Technology,* vol. 2, p. 110, 2012.

[14]  T.-S. Chung, L. Y. Jiang, Y. Li, and S. Kulprathipanja, "Mixed matrix membranes (MMMs) comprising organic polymers with dispersed inorganic fillers for gas separation," *Progress in Polymer Science,* vol. 32, pp. 483-507, 4// 2007.

[15]  M. Rezakazemi, A. Ebadi Amooghin, M. M. Montazer-Rahmati, A. F. Ismail, and T. Matsuura, "State-of-the-art membrane based CO2 separation using mixed matrix membranes (MMMs): An overview on current status and future directions," *Progress in Polymer Science,* vol. 39, pp. 817-861, 5// 2014.

[16]  J. J. Licari, "2.13.1 Chemistry," in *Coating Materials for Electronic Applications - Polymers, Processes, Reliability, Testing*, ed: William Andrew Publishing/Noyes.

[17]  P. S. Goh, A. F. Ismail, S. M. Sanip, B. C. Ng, and M. Aziz, "Recent advances of inorganic fillers in mixed matrix membrane for gas separation," *Separation and Purification Technology,* vol. 81, pp. 243–264, 2011.

[18]  T.-S. Chung, L. Y. Jiang, Y. Li, and S. Kulprathipanja, "Mixed matrix membranes (MMMs) comprising organic polymers with dispersed inorganic fillers for gas separation," *Progress in Polymer Science,* vol. 32, pp. 483-507, 2007.

[19]  A. F. Ismail, P. S. Goh, S. M. Sanip, and M. Aziz, "Transport and separation properties of carbon nanotube-mixed matrix membrane," *Separation and Purification Technology,* vol. 70, pp. 12–26, 2009.

[20]  D. Q. Vu, W. J. Koros, and S. J. Miller, "Mixed matrix membranes using carbon molecular sieves: I. Preparation and experimental results," *Journal of Membrane Science,* vol. 211, pp. 311-334, 2003.

[21]  M. Anson, J. Marchese, E. Garis, N. Ochoa, and C. Pagliero, "ABS copolymer-activated carbon mixed matrix membranes for CO2/CH4 separation," *Journal of Membrane Science,* vol. 243, pp. 19-28, 11/1/ 2004.

[22]  M. Anson, J. Marchese, E. Garis, N. Ochoa, and C. Pagliero, "ABS copolymer-activated carbon mixed matrix membranes for CO 2/CH4 separation," *Journal of Membrane Science,* vol. 243, pp. 19-28, 2004.

[23]  Y. Li, T.-S. Chung, and S. Kulprathipanja, "Novel Ag+-zeolite/polymer mixed matrix membranes with a high CO2/CH4 selectivity," *AIChE Journal,* vol. 53, pp. 610-616, 2007.

[24]  S. Kim, E. Marand, J. Ida, and V. V. Guliants, "Polysulfone and mesoporous molecular sieve MCM-48 mixed matrix membranes for gas separation," *Chemistry of Materials,* vol. 18, pp. 1149-1155, 2006.

[25]  S. Kim, L. Chen, J. K. Johnson, and E. Marand, "Polysulfone and functionalized carbon nanotube mixed matrix membranes for gas separation: Theory and experiment," *Journal of Membrane Science,* vol. 294, pp. 147-158, 2007.

[26]  E. V. Perez, K. J. Balkus Jr, J. P. Ferraris, and I. H. Musselman, "Mixed-matrix membranes containing MOF-5 for gas separations," *Journal of Membrane Science,* vol. 328, pp. 165-173, 2009.

[27]  Y. Zhang, K. J. Balkus Jr, I. H. Musselman, and J. P. Ferraris, "Mixed-matrix membranes composed of Matrimid® and mesoporous ZSM-5 nanoparticles," *Journal of Membrane Science,* vol. 325, pp. 28-39, 2008.

[28]  Y. Zhang, I. H. Musselman, J. P. Ferraris, and K. J. Balkus Jr, "Gas permeability properties of Matrimid® membranes containing the metal-organic framework Cu-BPY-HFS," *Journal of Membrane Science,* vol. 313, pp. 170-181, 2008.

[29]  T. S. Chung, S. S. Chan, R. Wang, Z. Lu, and C. He, "Characterization of permeability and sorption in Matrimid/C60 mixed matrix membranes," *Journal of Membrane Science,* vol. 211, pp. 91-99, 2003.

[30] D. Sen, H. Kalipcilar, and L. Yilmaz, "Development of zeolite filled polycarbonate mixed matrix gas separation membranes," *Desalination,* vol. 200, pp. 222-224, 2006.

[31] D. Şen, H. Kalipçilar, and L. Yilmaz, "Development of polycarbonate based zeolite 4A filled mixed matrix gas separation membranes," *Journal of Membrane Science,* vol. 303, pp. 194-203, 2007.

[32] A. Car, C. Stropnik, and K. V. Peinemann, "Hybrid membrane materials with different metal-organic frameworks (MOFs) for gas separation," *Desalination,* vol. 200, pp. 424-426, 2006.

[33] P. Jha and J. D. Way, "Carbon dioxide selective mixed-matrix membranes formulation and characterization using rubbery substituted polyphosphazene," *Journal of Membrane Science,* vol. 324, pp. 151-161, 2008.

[34] J. Ahn, W. J. Chung, I. Pinnau, and M. D. Guiver, "Polysulfone/silica nanoparticle mixed-matrix membranes for gas separation," *Journal of Membrane Science,* vol. 314, pp. 123-133, 2008.

[35] Y. Li, T. S. Chung, Z. Huang, and S. Kulprathipanja, "Dual-layer polyethersulfone (PES)/BTDA-TDI/MDI co-polyimide (P84) hollow fiber membranes with a submicron PES-zeolite beta mixed matrix dense-selective layer for gas separation," *Journal of Membrane Science,* vol. 277, pp. 28-37, 2006.

[36] T. H. Bae, L. Junqiang, S. L. Jong, W. J. Koros, C. W. Jones, and S. Nair, "Facile high-yield solvothermal deposition of inorganic nanostructures on zeolite crystals for mixed matrix membrane fabrication," *Journal of the American Chemical Society,* vol. 131, pp. 14662-14663, 2009.

[37] R. Adams, C. Carson, J. Ward, R. Tannenbaum, and W. Koros, "Metal organic framework mixed matrix membranes for gas separations," *Microporous and Mesoporous Materials,* vol. 131, pp. 13-20, 2010.

[38] Y. Li, T. S. Chung, and S. Kulprathipanja, "Novel Ag+-zeolite/polymer mixed matrix membranes with a high CO2/CH4 selectivity," *AIChE Journal,* vol. 53, pp. 610-616, 2007.

[39] Y. Zhang, I. H. Musselman, J. P. Ferraris, and K. J. Balkus Jr, "Gas permeability properties of mixed-matrix matrimid membranes containing a carbon aerogel: A material with both micropores and mesopores," *Industrial and Engineering Chemistry Research,* vol. 47, pp. 2794-2802, 2008.

[40] B. Zornoza, C. Téllez, and J. Coronas, "Mixed matrix membranes comprising glassy polymers and dispersed mesoporous silica spheres for gas separation," *Journal of Membrane Science,* vol. 368, pp. 100-109, 2011.

[41] B. Zornoza, O. Esekhile, W. J. Koros, C. Téllez, and J. Coronas, "Hollow silicalite-1 sphere-polymer mixed matrix membranes for gas separation," *Separation and Purification Technology,* vol. 77, pp. 137-145, 2011.

[42] L. Li, T. Wang, Q. Liu, Y. Cao, and J. Qiu, "A high CO 2 permselective mesoporous silica/carbon composite membrane for CO 2 separation," *Carbon,* vol. 50, pp. 5186-5195, 2012.

[43] B. Zornoza, B. Seoane, J. M. Zamaro, C. Téllez, and J. Coronas, "Combination of MOFs and zeolites for mixed-matrix membranes," *ChemPhysChem,* vol. 12, pp. 2781-2785, 2011.

[44] S. Kim and E. Marand, "High permeability nano-composite membranes based on mesoporous MCM-41 nanoparticles in a polysulfone matrix," *Microporous and Mesoporous Materials,* vol. 114, pp. 129-136, 9/1/ 2008.

[45] I. Musselman, J. Kenneth Balkus, and J. Ferraris, "Mixed-Matric Membranes for CO2 and H2 Gas Separations Using Metal-Organic Framework and Mesoporus Hybrid Silicas," 2009.

[46] A. F. Ismail, P. S. Goh, S. M. Sanip, and M. Aziz, "Transport and separation properties of carbon nanotube-mixed matrix membrane," *Separation and Purification Technology,* vol. 70, pp. 12-26, 11/19/ 2009.

[47] S. E. Lehman and S. C. Larsen, "Zeolite and mesoporous silica nanomaterials: greener syntheses, environmental applications and biological toxicity," *Environmental Science: Nano,* vol. 1, pp. 200-213, 2014.

[48] A. R. S. A. S. Yusup, "Effect of monoethanolamine loading on the physicochemical properties of amine-functionalized Si-MCM-41," *Sains Malaysiana,* vol. 43, pp. 253-259, 2014.

[49]    B. D. Reid, F. A. Ruiz-Trevino, I. H. Musselman, K. J. Balkus Jr, and J. P. Ferraris, "Gas permeability properties of polysulfone membranes containing the mesoporous molecular sieve MCM-41," *Chemistry of Materials,* vol. 13, pp. 2366-2373, 2001.

[50]    N. S. O. Bakhtiari, "The Formed Voids around the Filler Particles Impact on the MMM," *International Journal of Chemical Engineering and Applications,* vol. 5, pp. 198-203, 2014.

[51]    J. García-Martínez and E. J. Moniz, *Nanotechnology for the Energy Challenge*: Wiley, 2010.

[52]    N. I. T. S. E. M. N. Katun, "Functionalization of Mesoporous Si-MCM-41 by Grafting with Trimethylchlorosilane," *International Journal of Chemistry,* vol. 3, August 2011 2011.

[53]    S. Kim, J. Ida, V. V. Guliants, and J. Y. S. Lin, "Tailoring pore properties of MCM-48 silica for selective adsorption of CO 2," *Journal of Physical Chemistry B,* vol. 109, pp. 6287-6293, 2005.

[54]    "(3-Aminopropyl)triethoxysilane 99%," (3-Aminopropyl)triethoxysilane, Ed., ed. Sigma-Aldrich: Sigma-Aldrich Co.

[55]    Sigma-Aldrich,        "(3-Aminopropyl)trimethoxysilane,"        -.        (3-Aminopropyl)trimethoxysilane,                Ed.,                ed. http://www.sigmaaldrich.com/catalog/product/aldrich/281778?lang=en&region= MY: Sigma-Aldrich, 2013.

[56]    "[3-(2-Aminoethylamino)propyl]trimethoxysilane,"                [3-(2-Aminoethylamino)propyl]trimethoxysilane, Ed., ed. Sigma-Aldrich: Sigma-Aldrich Co.

[57]    A. F. Ismail and P. Y. Lai, "Development of defect-free asymmetric polysulfone membranes for gas separation using response surface methodology," *Separation and Purification Technology,* vol. 40, pp. 191-207, 12/1/ 2004.

[58]    M. U. M. Junaidi, C. P. Leo, A. L. Ahmad, S. N. M. Kamal, and T. L. Chew, "Carbon dioxide separation using asymmetric polysulfone mixed matrix membranes incorporated with SAPO-34 zeolite," *Fuel Processing Technology,* vol. 118, pp. 125-132, 2// 2014.

[59]    S. Kim, "High Permeability/High Diffusivity Mixed Matrix Membranes For Gas Separations," PhD, Chemical Engineering, Virginia Polytechnic Institute and State University, Blacksburg, VA, 2007.

[60]    Z. Hamzah, N. Narawi, H. M. Rasid, A. N. Yusoff, "Synthesis And Characterization Of Mesoporous Material Functionalized With Different Silylating Agent And Their Capability To Remove Cu2+," *The Malaysian Journal of Analytical Sciences,* vol. 16, pp. 290-296, 2012.

[61]    K. M. Parida and D. Rath, "Amine functionalized MCM-41: An active and reusable catalyst for Knoevenagel condensation reaction," *Journal of Molecular Catalysis A: Chemical,* vol. 310, pp. 93-100, 9/1/ 2009.

[62]    M. A. Aroon, A. F. Ismail, M. M. Montazer-Rahmati, and T. Matsuura, "Morphology and permeation properties of polysulfone membranes for gas separation: Effects of non-solvent additives and co-solvent," *Separation and Purification Technology,* vol. 72, pp. 194-202, 4/20/ 2010.

[63]    Y. Zhang, J. Sunarso, S. Liu, and R. Wang, "Current status and development of membranes for CO2/CH4 separation: A review," *International Journal of Greenhouse Gas Control,* vol. 12, pp. 84-107, 1// 2013.

[64]    H. I. Meléndez-Ortiz, Y. Perera-Mercado, J. A. Mercado-Silva, Y. Olivares-Maldonado, G. Castruita, and L. A. García-Cerda, "Functionalization with amine-containing organosilane of mesoporous silica MCM-41 and MCM-48 obtained at room temperature," *Ceramics International,* vol. 40, pp. 9701-9707, 8// 2014.

## APPENDIX I - CALCULATION

## Calculation for pure Psf membrane

| Chemical | wt% | Density (g/mL) |
|---|---|---|
| Polysulfone (Psf) | 25.00 | 1.240 |
| N-Methyl-2-pyrrolidone (NMP) | 75.00 | 1.028 |

Volume (mL) of each component needed to synthesize about 13 g of membrane. A membrane volume of about 12mL is needed for each membrane casting.

$$\text{Volume of each component} = \frac{13\,\text{g} \times \text{wt\%}/100}{\text{density of component}}$$

Mass of component = volume of component × density of component

| Chemical | Volume (mL) | Mass (g) | Membrane volume (mL) | Membrane mass (g) |
|---|---|---|---|---|
| PSf | $\frac{13 \times 0.25}{1.240} = 2.621$ | 2.621 x 1.24 = 3.250g | 2.621 + 9.484 = 12.105 mL | 25 + 9.75 = 13 g |
| NMP | $\frac{13 \times 0.75}{1.028} = 9.484$ | 9.484 x 1.028 = 9.750 | | |

**Calculation of Permeability (GPU conversion to Barrer)**

Take $CO_2$ permeance = 35.53 GPU for pure Psf membrane

$GPU = 1 \times 10^{-6}$ cm³ (STP) /cm²s cm Hg

$Barrer = 1 \times 10^{-10}$ cm³ (STP) cm/cm²s cm Hg

Membrane thickness = 25 μm = 0.0025 cm

$$Permeability = \frac{35.53 \times 10^{-6} cm^3 \ (STP) \ /cm^2 s \ cm \ Hg \times 0.0025 \ cm}{10^{-4}}$$

$\qquad\qquad$ = 888.25 cm³ (STP) cm/cm²s cm Hg

$\qquad\qquad$ = 888.25 Barrer

**Table 14: Conversion of unit for membrane permeability (GPU to Barrer)**

| Loading % (w/w) | Type of fillers | $CO_2$ Permeability | | Ideal selectivity α($CO_2$/$CH_4$) |
|---|---|---|---|---|
| | | GPU | Barrer | |
| 0 | - | 35.53 | 888.25 | 1.19 |
| 0.1 | MCM-41 | 76.07 | 1901.75 | 0.72 |
| | APTMS-MCM-41 | 181.36 | 4534.00 | 0.73 |
| | AAPTMS-MCM-41 | 21.94 | 548.50 | 1.39 |
| 1 | MCM-41 | 100.41 | 2510.25 | 0.62 |
| | APTMS-MCM-41 | 238.04 | 5951.00 | 0.68 |
| | AAPTMS-MCM-41 | 145.43 | 3635.75 | 0.64 |

The data in Table 14 is used to plot the graph of ideal selectivity vs permeability (Barrer) (shown in Figure 23).

**APPENDIX II – PROCEDURE OF SYNTHESIS OF MCM-41**

The experiment has been started with the synthesis of pure MCM-41 and Table 15 describes the overall synthesis process.

**Table 15: Synthesis of MCM-41 particles**

| Observation | Description |
|---|---|
|  | Heating and stirring the particles solution at 80°C |
|  | Centrifugation to recover and wash the particles at 8000 rpm |
|  | Drying collected particles (after centrifugation) overnight in oven at 100°C |
|  | Observation after drying in oven |

| | |
|---|---|
|  | Calcination using furnace at 500°C for 10 h |
|  | Particles collected are stored in airtight container |
|  | Grinding MCM-41 particles into fine powder using mortar. |